Remote Sensing of Environment 260 (2021) 112477

Contents lists available at ScienceDirect

Remote Sensing of Environment

journal homepage: www.elsevier.com/locate/rse

Modelling lidar-derived estimates of forest attributes over space and time: A review of approaches and future trends

Nicholas C. Coops [a,*], Piotr Tompalski [a], Tristan R.H. Goodbody [a], Martin Queinnec [a], Joan E. Luther [b], Douglas K. Bolton [c], Joanne C. White [d], Michael A. Wulder [d], Oliver R. van Lier [e], Txomin Hermosilla [d]

[a] Integrated Remote Sensing Studio, Department of Forest Resources Management, University of British Columbia, 2424 Main Mall, Vancouver, BC V6T1Z4, Canada
[b] Canadian Forest Service (Atlantic Forestry Centre), Natural Resources Canada, 26 University Drive, Corner Brook, NL A2H 5G4, Canada
[c] Department of Earth & Environment, Boston University, 685 Commonwealth Avenue, Boston, MA 02215, USA
[d] Canadian Forest Service (Pacific Forestry Centre), Natural Resources Canada, 506 West Burnside Road, Victoria, BC V8Z1M5, Canada
[e] Canadian Forest Service (Canadian Wood Fibre Centre), Natural Resources Canada, 26 University Drive, Corner Brook, NL A2H 5G4, Canada

ARTICLE INFO

Editor: Jing M. Chen

Keywords:
Large area
Airborne lidar
Spaceborne lidar
GEDI
ICESat

ABSTRACT

Light detection and ranging (lidar) data acquired from airborne or spaceborne platforms have revolutionized measurement and mapping of forest attributes. Airborne data are often either acquired using multiple overlapped flight lines to provide complete coverage of an area of interest, or using transects to sample a given population. Spaceborne lidar datasets are unique to each sensor and are sample- or profile-based with characteristics driven by acquisition mode and orbital parameters. To leverage the wealth of accurate vegetation structural data from these lidar systems, a number of approaches have been developed to extend these observations over broader areas, from local landscapes to the globe. In this review we examine studies that have utilised modelling approaches to extend air- or space-based lidar data with the aim of communicating methods, outcomes, and accuracies, and offering guidance on linking lidar metrics and lidar-derived forest attributes with broad-area predictors. Modelling approaches are developed for a variety of applications. In some cases, generation of spatially-exhaustive layers may be useful for forest management purposes, driving management and inventory decisions over smaller focus areas or regions. In other cases, outputs are designed for monitoring at regional or global scales, and may be – due to the spatial grain of the structural estimates – insufficiently accurate or reliable for management. From the reviewed studies, we found height, aboveground biomass and volume, derived from either upper proportions of a large-footprint full-waveform lidar profiles, or statistically modelled from discrete return small-footprint lidar point clouds, to be the most commonly extended forest attributes, followed by canopy cover, basal area and stand complexity. Assessment of the accuracy and bias of the extrapolated forest attributes varied with both independent and model-derived estimates. The coefficient of determination (R^2) was the most often reported, followed by absolute and relative (i.e., as a proportion of the mean) root mean square error (RMSE and RMSE% respectively). Compilation of the stated accuracies suggested that the variance explained in predictions of forest height ranged from $R^2 = 0.38$ to 0.90 (mean = 0.64), RMSE from 2 to 6m and RMSE% from 12 to 34%. For volume, R^2 ranged from 0.25 to 0.72 (mean = 0.53) and RMSE from 60 to 87 m^3/ha and for aboveground biomass (AGB) R^2 ranged from 0.35 to 0.78 (mean = 0.55) and RMSE from 28 to 44 Mg/ha. There was no consensus on the level of accuracy required to support successful extension over larger areas. Ultimately, the review suggests that the information need motivating the spatial extension over larger areas drives the choice of the type of lidar data, spatial datasets and related grain. We conclude by discussing future directions and the outlook for new approaches including new lidar-derived response variables, advances in modelling approaches, and assessment of change.

* Corresponding author.
E-mail address: nicholas.coops@ubc.ca (N.C. Coops).

https://doi.org/10.1016/j.rse.2021.112477
Received 16 November 2020; Received in revised form 18 April 2021; Accepted 24 April 2021
Available online 1 May 2021

1. Introduction

1.1. Extending forest attribute information over space

Demand for spatially-explicit and synoptic forest attribute data is continually growing to meet an ever-increasing suite of management, reporting, and research information needs. Over the last decade, requirements for information describing forested landscapes has grown, with global, national and local agencies all seeking precise and accurate spatially-explicit information on forest resources (Næsset, 2014; Magnussen et al., 2018). Forest biomass, for example, is recognised by the Global Climate Observing Systems as an Essential Climate Variable (Duncanson et al., 2019) and its systematic characterization is important for reporting on afforestation, reforestation, and deforestation categories globally (Herold et al., 2019). As a result, regional and global products suitable for monitoring are required at sufficiently fine spatial scales and at an adequate level of accuracy to observe changes in forest ecosystems as driven by both natural and anthropogenic activities. These estimates then provide policy makers with enhanced knowledge of carbon resources, regional biodiversity, and improved strategies for sustainable resource development (Duncanson et al., 2019). In contrast, regional and local spatially- explicit information on attributes such as forest volume and height are the cornerstone of enhanced forest inventories (White et al., 2013), and are required to meet forest stewardship responsibilities (White et al., 2016), at operational and tactical planning levels. In these cases, the coverage of the resultant products is generally more spatially limited in scope, with a more refined list of forest attributes, and with higher accuracy requirements to support forest inventory and other management scale decision making. Whether for global monitoring or local management, forest characterization approaches based upon remotely sensed data have benefits including the capacity to predict forest attributes across all forests, and they are not spatially limited to areas captured in forest inventory programs or the related compilation time step (Wulder et al., 2020). Likewise, predicted attributes can include a wide range of forest attributes including aboveground biomass (AGB), height, volume, crown cover and canopy complexity, with applications ranging from habitat assessment, species distributions, informing fire risk and fire severity among many others.

1.2. Light detection and ranging

The rapid uptake of light detection and ranging (lidar) technologies on a variety of acquisition platforms (see Table 1 for a summary of lidar platforms relevant to this review) has revolutionized the capture of forest structure information through the acquisition of precise three dimensional information. The technology is highly adaptive with ground (or terrestrial), unmanned aerial systems (UAS), and aircraft- or satellite-based instruments, all successfully being applied to extract a range of forest structural attributes at varying spatial scales (White et al., 2016). In general, lidar has seen rapid development from scientific tests to operational application (Nelson, 2013) with associated costs going down concurrent with an increase in sensors available and acquisition platforms/scenarios (Table 1).

Airborne laser scanning systems, including systems with lidar mounted on an aircraft (ALS) or on a UAS, use the returned energy from emitted laser pulses to describe the three dimensional structure of aboveground vegetation. Airborne systems come in a variety of configurations (White et al., 2016). Small footprint ALS systems typically record between 1 and 5 returns per laser pulse in discrete mode, or a fully digitized vertical profile of the returned energy in full-waveform mode (Wulder et al., 2008, 2013). Typically, these systems produce footprint sizes of 0.1–2 m (Wulder et al., 2008; Lim et al., 2003) and can achieve sub-meter accuracy of terrain surface heights (Blair et al., 1999; Lefsky et al., 2002). Large footprint lidar systems utilise a different approach (Lefsky et al., 2002). A key example, NASA's Land, Vegetation, and Ice Sensor (LVIS) has a footprint size that can vary between 10 and 80 m in diameter, with a 25 m footprint typically used as shown by Drake et al. (2002). The footprint depends on the altitude of the aircraft (Lim et al., 2003), with the instrument recording the full waveform of the reflected laser pulse. The number of aircraft-based, large-footprint systems is limited, and these systems are often used to simulate space-based measurements. Satellite laser sensors such as the Geoscience Laser Altimeter System (GLAS) onboard the Ice, Cloud and land Elevation Satellite (ICESat) acquired global waveform data between 2003 and 2009. The data produced by the GLAS instrument varied over the life of the mission associated with changes in laser power and as a result, the far field illumination changed over time. However, the instrument provided a pathfinder set of satellite-based lidar measurements with a

Table 1
Summary of lidar instruments and platforms relevant for this review.

LiDAR Platform	Sensor	Recording mode	Acquisition strategy	Wavelength	Footprint size	Spatial extent	Notes
Spaceborne	GLAS (ICESat satellite)	Full waveform	Sampling (1 footprint every 170 m along laser ground track)	532 nm/1064 nm	~70 m	Global (± 86° N/S latitude)	Slope effect limitations on terrain height retrieval
	ATLAS (ICESat-2 satellite)	Photon-sensitive discrete returns	Profiling (1 footprint every 70 cm along laser ground track)	532 nm	~14 m	Global (± 88° N/S latitude)	
	GEDI (ISS)	Full waveform	Sampling (1 footprint every 60 m along ground track)	1064 nm	~25 m	Near-Global (± 51.6° N/S latitude)	Limited in extent by ISS orbit
Airborne	Overview of multiple conventional linear mode systems	Discrete returns	Scanning or profiling	800–2500 nm (Near-Infrared range)	10–30 cm at 500–3000 m range	Regional to country scale	
	Land, Vegetation and Ice Sensor (LVIS)	Full waveform	Scanning	1064 nm	20–30 m	Regional to country scale	Limited to 1 instrument operated by NASA
	SPL100 (Leica/ Hexagon)	Photonsensitive discrete returns	Scanning	532 nm	20–30 cm at 3000–4000 m range	Regional to country scale	Potential canopy penetration and ground retrieval limitations under dense vegetation (Brown et al., 2020)
UAS	Overview of multiple conventional systems	Discrete returns	Scanning	700 nm	2.5–30 cm at 50 m – 100 m range	Local	Plot and landscape deployments due to operational and power constraints

Acronyms used: Advanced Topographic Laser Altimeter System (ATLAS); Global Ecosystem Dynamics Investigation (GEDI); Geoscience Laser Altimeter System (GLAS); Ice, Cloud and Land Elevation Satellite (ICESat); International Space Station (ISS); unmanned aerial systems (UAS).

nominal 90-m footprint that have been applied to vegetation and forest studies globally (Abshire et al., 2005). Most recently, two additional spaceborne lidar systems have been launched and are acquiring lidar data. Specifically, the full-waveform Global Ecosystem Dynamics Investigation (GEDI) on the International Space Station (ISS) and a single photon lidar (SPL) system on ICESat-2/ATLAS now provide valuable space-based data for forest assessments (Hancock et al., 2019; Markus et al., 2017).

1.3. Current limitations of lidar-based forest attribute estimation

While providing highly-detailed and precise, spatially-explicit information on the structure of forest vegetation, characterization of forest stands using lidar technology over areas requires consideration of a number of sampling, statistical, and methodological constraints. In some countries, coordinated national lidar acquisitions have been implemented as shown by Kotivuori et al. (2016) and Magnussen et al. (2018), and some large forested regions within nations likewise have systematic lidar acquisition campaigns as shown by Fradette et al. (2019). Often however, lidar surveys are intended to provide detailed data, in specific targeted areas and acquisitions vary with respect to sensor types, phenology (leaf on and leaf off), and year of acquisition. Spaceborne laser systems, while global or near global in scope, are sample based, requiring a degree of gridding to produce attributes over spatially-contiguous regions of forest. In contrast, UAS-based systems provide exceptional detail over very small target acquisition areas (Goodbody et al., 2017). As a result, the information extracted from lidar datasets also differs with sub crown level information possible using UAS and low aircraft acquisitions through to plot or stand level summaries from higher altitude airborne and spaceborne platforms. Accuracy for the prediction of tree and stand level attributes typically differs as a function of lidar footprint size, data density, and coverage.

Wulder et al. (2012a) reviewed the large-area characterization of forest resources with focus on the use of lidar technology as a sampling tool for large area estimation. In that review, issues such as sample design, statistical models, and estimation approaches were discussed. Looking forward, Wulder et al. (2012a) described that not all characterisations of large areas can be satisfied with sample-based statistical characterizations of a given population and that spatially-explicit mapping of vertical structure is often required. While examples were limited at the time of this earlier review, the authors indicated that lidar offered a valuable source of calibration and validation data to augment mapping efforts, and that the use of samples of lidar (known as "lidar plots"; Wulder et al., 2012b) would improve the ability to map biophysical variables in an accurate, spatially-explicit, and economically-viable fashion. Synoptic optical imagery or Radio Detection and Ranging (RADAR) with appropriate spatial resolutions offer a means to model and map forest vertical structure from lidar plots (Wulder et al., 2012b). Three dimensional characteristics can be modelled directly or forest structure attributes can be predicted, providing independent calibration and validation data for model extrapolations (Hudak et al., 2002; Zald et al., 2016). Incorporating lidar plots could improve the accuracy of conventional optical image or RADAR-based estimates over larger areas (e.g., $>$ 10 million ha). Wulder et al. (2012a) concluded that through the integration of spatially-exhaustive optical and spatially-limited samples of lidar data, forest attribute estimation in support of national and international reporting may be generated. Given the rapid progress in lidar remote sensing of forests, the earlier identified promise is now a reality, with sufficient literature examples enabling a focused review of spatial modelling of lidar captured forest structure over larger areas.

1.4. Aim of the review

The overall goal of this communication is to review the recent progress in extending airborne lidar-based metrics or lidar-derived forest attribute estimates to broader forested landscapes where spatially-exhaustive passive (e.g. optical) or active (RADAR) satellite data are available. To do so, we open with a conceptual description of the modelling process. We then describe the most established lidar-based metrics or lidar-derived forest attributes and the predictor variables used, in turn, to enable extension over the broader region of interest. Next, we describe the statistical approaches used to develop relationships between lidar-based response variables and wall-to-wall (i.e. spatially exhaustive) predictors, followed by an examination of accuracy assessment approaches for modelling techniques. We conclude by discussing future directions, including the availability of new lidar-based response variables, advances in modelling approaches, and expanded capabilities for the assessment of forest change.

2. Review of modelling studies to extend lidar-derived estimates over space

2.1. Conceptual development

The utilisation of multiple sources of remote sensing observations with field data is common in forest inventories as this combination offers cost effective estimation opportunities and capacity for regular update of observations over broad landscapes. The process of creating a wall-to-wall coverage from spatially-dispersed sample areas is generally referred to as interpolation, whilst extending from a limited number of samples to a larger spatial extent is extrapolation (Miller et al., 2004). In the remote sensing literature, additional terms such as "prediction" or "scaling up" have also been used. We reviewed papers that were published using any of these terms in association with the terms "lidar", "laser scanning", or "point cloud", to inform this review. We only considered studies where lidar-based metrics (including point-derived metrics, such as mean height, height percentiles, variance, or proportion of returns; and full-waveform metrics such as Height of Median Energy (HOME) or lidar-derived forest attributes (such as estimates of volume, cover, and biomass) were extrapolated to new locations or, less commonly, different temporal periods, using models followed by some degree of validation. Those published studies that informed our review are shown in Table 2.

From a statistical viewpoint, the use of remotely-sensed data to extend information to a different area or time period is a model-based approach (Saarela et al., 2016) based on the concept of a super population, with the super population defined as the innumerable population from which samples are drawn (Cassel et al., 1977), and in this paper would refer to the broader area across which estimates are to be extrapolated. Within this population of cells, a sample is acquired using lidar data, which could be collected in transect(s) or as a spatially-complete area over a smaller subset of the broader area of interest as shown by Bolton et al. (2018). Within that sample, a further refined subset will have ground-based field observations (i.e., from established field visited ground plots), which may include measurements of height, cover, biomass, volume and so on. Ultimately, the model-based survey at this finest scale aims for a population mean that corresponds to the expected mean of the super population (Ståhl et al., 2016).

Saarela et al. (2016) outline key modelling approaches used with remotely sensed data: standard model-based inference, hybrid inference, and model-based inference with hierarchical modelling. Relationships developed directly between the more broad spatially exhaustive observations and the ground-based field data are known as standard model-based inference, which has no assumption on the probabilities of inclusion of samples. In other words we only assume the samples come from the same super population and we can select from any acquisition program we wish, for example from a transect or profile and so on. In two phase model-based estimation, lidar data are available for a portion of the area, and models are developed to extrapolate the lidar based metrics or lidar derived forest attributes to the broader area. When lidar based metrics are extrapolated using two phase model-based

Table 2
Studies forming the basis of the review.

Author	Location	Lidar data used	Lidar-based metric or lidar-derived forest attribute	Method for lidar-derived attribute prediction	Accuracy field vs lidar	Predictors	Method for extension	Grid-cell size and spatial extent of study area	Independent error assessment	Accuracy of extended attributes
Andersen et al. (2012)	Interior Alaska, USA	ALS	Total Biomass	Regression	$R^2 = 0.74$	Landsat TM/ ETM+ and PALSAR	k-NN Imputation	18 m 2012 km^2	None	Relative standard error 5.1%
Badreldin and Sanchez-Azofeifa (2015)	Alberta, Canada	ALS	AGB	Multiple Linear Regression	$R^2 = 0.74$	Landsat ETM+	Multiple Linear Regression	30 m 70 km^2	None	$R^2 = 0.78$; RMSE = 44 Mg/ha
Bolton et al. (2020)	Canada	ALS	Height, Basal Area and Net Volume	Unknown	Unknown	Landsat TM/ ETM+	K-NN Imputation with random forest metric	30 m 3500km^2h	None	$R^2 =$ 0.54–0.66; RMSE = 16–34%
Cartus et al. (2012)	Chile	ALS	Canopy height, Volume	Random Forest	$R^2 =$ 0.81–0.93	ALOS PALSAR and Landsat ETM+	Random Forest	Variable seg. Size 6300 km^2	Independent	$R^2 =$ 0.72–0.87; RMSE% = 15–25%
Chi et al. (2015)	China	ICESat GLAS	AGB	Multiple Regression	$R^2 =$ 0.63–0.90	MODIS Reflectance, VCF and SRTM elevation	Multiple Regression	500 m 9.6 M km^2	None	$R^2 =$ 0.43–67; RMSE = 8–28 Mg/ ha^{-1}
Hudak et al. (2002)	Oregon USA	ALS	Maximum Canopy Height	NA	NA	Landsat ETM+	Geostatistics	25 m 200 km^2	None	$r = 0.86$ with 250 m point samples
Hyde et al. (2006)	Sierra Nevada USA	LVIS	Canopy Height, Max Height, Var Height, AGB	Multiple Regression	$R^2 =$ 0.59–0.76	Landsat ETM/ X-Band SAR/ INSAR/ QuickBird	Multiple Regression	100 m 600 km^2	None	At 50% sample canopy height $R^2 =$ 0.41, AGB $R^2 = 0.35$
Kellndorfer et al. (2010)	Eastern USA	LVIS	Lidar Waveform Height	NA	NA	SRTM INSAR. Landsat ETM Land Cover	Random Forest	Seg. mean = 130 m 110,000 km^2	Independent	$r = 0.71$ RMSE = 4.4 m
Lefsky (2010)	Global	ICESat/ GLAS	90th % LiDAR height	NA	NA	MODIS	Cubist regression model	Seg. mean = 500 m Globe	None	$R^2 = 0.67$, RMSE = 5.9 m
Li et al. (2016)	Northwestern China	ALS	AGB	Regression	$R^2 = 0.78$	ALOS PALSAR	Regression/ Non parametric models	30 m 130 km^2	Independent	$R^2 = 0.65$ RMSE = 28.3 Mg/ha
Luther et al. (2019)	Newfoundland, Canada	ALS	Height, Basal Area, Volume, and AGB	Random Forest and Regression	$R^2 =$ 0.9–0.95	Sentinel 2/ ALOS PALSAR	Random Forest/ Subset Regression	20 m 5600 km^2	Independent	$R^2 =$ 0.56–0.84. RMSE 16–36%
Mahoney et al. (2018)	Northwest Territories, Canada	ALS and ICESat GLAS	Height and Crown Closure	Regression	$R^2 =$ 0.63–0.89	Landsat TM, Climate, Terrain, Land Cover	k-NN Imputation	30 m 200,000 km^2	Independent	Heights within 7%, Canopy Cover within 11%
Margolis et al., 2015	North America	Airborne PALS	AGB	Multiple Linear Regression	$R^2 =$ 0.58–0.8	ICESat GLAS/ Land Cover	Multiple Linear Regression	25 m 36 M km^2	Independent	Relative difference 7.0–44.7%
Maselli et al. (2011)	Central Italy	ALS	Volume	Regression	$r = 0.62$	Landsat ETM+	K-NN Imputation	10 m, ANS	Independent	$r = 0.85$, RMSE = 59.2 m3/ha
Matasci et al. (2018a)	Boreal Forested ecosystems of Canada	ALS	Height, Height Var., Basal Area, Volume, and AGB.	Regression	$R^2 =$ 0.64–0.84	Landsat TM/ ETM+	K-NN Imputation with random forest metric	30 m >5.5 M km^2	Independent	$R^2 =$ 0.38–0.76 RMSE% = 18–38%
McInerney et al. (2010)	Scotland	ALS	Canopy Height	Regression	Mean deviation 1.36 m	Indian Resource Satellite - 1C	K-NN Imputation	20 m 115 km^2	Independent	RMSE = 28–31%
Montesano et al. (2013)	Maine, USA	LVIS	AGB	Regression	$R^2 = 0.82$	ALOS PALSAR L-band SAR, Landsat ETM+	Random Forest	Seg mean = 2.5 ha 4030 km^2	None	$R^2 = 0.62$, RMSE = 41 Mg/ha

(continued on next page)

Table 2 (*continued*)

Author	Location	Lidar data used	Lidar-based metric or lidar-derived forest attribute	Method for lidar-derived attribute prediction	Accuracy field vs lidar	Predictors	Method for extension	Grid-cell size and spatial extent of study area	Independent error assessment	Accuracy of extended attributes
Pascual et al. (2010)	Central Spain	ALS	Lidar Mean, Median and variance	NA	NA	Landsat ETM+	Multiple Regression	30 m 1.28 km^2	None	R^2 = 0.62–0.66
Puliti et al. (2018)	Norway	ALS, UAS	Growing Stock Volume	Regression	R^2 = 0.83	Sentinel-2	Regression; hierarchical model-based inference	10 m 73.30 km^2	None	R^2 = 0.30 RMSE% = 37.47%,
Saarela et al. (2016, 2018)	Finland	ALS	Growing Stock Volume	Unknown	Unknown	Landsat	Regression; hierarchical model-based inference	16 m 300 km^2	None	R^2 = 0.25, RMSE = 79 m^3/ha
Simard et al. (2011)	Global	ICESat/ GLAS	LiDAR Maximum Height	NA	NA	MODIS Forest Type and Cover, Climate and Elevation	Regression Tree - Random Forest	1000 m 60°S-60°N	Independent	R^2 = 0.69, RMSE = 4.4 m
Stojanova et al. (2010)	Slovenia	ALS	Height, Canopy Cover	NA	NA	Landsat ETM+	9 machine learning algorithms	25 m 722 km^2	None	Height R^2 = 0.90; RMSE = 2.1 m. CC R^2 = 0.88, RMSE 14%
Sun et al. (2011)	Maine, USA	LVIS	AGB	Linear Regression	R^2 = 0.71	ALOS PALSAR L-band SAR	Linear Regression	75 m 100 km^2	None	R^2 = 0.63–0.71, RMSE = 28.2 Mg/ha
Urbazaev et al., 2018	Mexico	ALS	AGB	Regression	R^2 = 0.68	ALOS PALSAR L-band SAR, Landsat optical data and SRTM Terrain	Cubist Machine Learning	100 m 650,000 km^2	Independent	R^2 = 0.37, RMSE = 34.5 m^3/ha

Acronyms used: Aboveground Biomass (AGB); Airborne Laser Scanner (ALS); Advanced Land Observing Satellite (ALOS); Airborne LVIS instrument (Air LVIS), Enhanced Thematic Mapper (ETM+); Geoscience Laser Altimeter System (GLAS); Ice, Cloud and Land Elevation Satellite (ICESat); Interferometric Synthetic Aperture Radar (InSAR); Land, Vegetation, and Ice Sensor (LVIS); Moderate Resolution Imaging Spectroradiometer (MODIS); Segment size (Seg Size), Shuttle RADAR Terrain Mission (SRTM), Phased Array Type L-band Synthetic Aperture Radar (PALSAR); Portable Airborne Laser System (PALS); Root Mean Square Error (RMSE); Synthetic Aperture Radar (SAR); Thematic Mapper (TM); Vegetation Continuous Field (VCF). For the extent of the area of the prediction ANS: Area not specified. Independent error assessment is the use of independent field data, not used in either the lidar-based metric or lidar-derived forest attribute estimation or for the imputation.

estimation, this is known as hybrid inference which is a mix of design-based and model-based estimation frameworks (Ståhl et al., 2016). Cases where lidar and field data are first used to model key forest attributes (i.e., creating surrogate plots or lidar-plots (Wulder et al., 2012b)), and then using those predicted values for a given attribute as the response variable in a model, with which are then extrapolated to the spatially exhaustive layers as predictors, are referred to as an example of model-based inference with hierarchical modelling. All of the papers reviewed in this study fall within these last two estimation approaches, being examples of either hybrid inference or model-based inference with hierarchical modelling. An understanding of the underlying approach is critical, because if model error at one stage of the process is ignored, then the overall uncertainty of the model is unknown, and it can be expected that the variance of the final estimates that are reported are likely to be substantially underestimated as a result of the propagation of error, which may be as much as 70% (Saarela et al., 2016).

2.2. Lidar-based response variables

For clarity, we use the term lidar-based metrics to describe attributes of the full waveform, or the point cloud, which are to be extended over the broader spatial extent. In the case of full-waveform data, direct metrics from spaceborne sensors such as maximum full-waveform return height or proportions of return energy have been shown to correlate well with stand height (Lefsky, 2010). From small-footprint lidar point-cloud data, forest height and cover attributes have been found to be directly correlated with lidar-based metrics without any additional modelling. For example, Pascual et al. (2010) extrapolated summaries of airborne lidar-based metrics including the mean, median, and standard deviation of the ALS return heights derived from 30-m grid cells—corresponding to the dimensions of Landsat pixels— over a demonstration area in central Spain. Similarly, Stojanova et al. (2010) derived ALS estimates of forest height (mean lidar return height) and canopy cover (% returns > 1 m) for 25-m grid cells and extrapolated these metrics over a forested region in Slovenia. Matasci et al. (2018a) also extrapolated a number of lidar-based metrics including the mean, standard deviation, and 95th percentile as well as proportions of returns among others for > 5.5 M km^2 of Canadian boreal forest. In these studies using small-footprint ALS, the error associated with differences between the lidar-based metric (such as height or proportion of returns) and the forest attribute of interest (e.g. stand height) is assumed to be negligible. Among the studies reviewed (Table 2), the most commonly extrapolated lidar-based metrics were height related, followed by the proportion of returns above a defined height, which is used as a surrogate for canopy cover.

Lidar-based metrics are commonly used to model key forest attributes such as aboveground biomass (AGB) and volume and provide more refined and locally-calibrated forest attributes over an area of interest. In this review, we refer to these as lidar-derived forest attributes.

This approach forms a model-based inference with hierarchical modelling approach and has been commonly applied, especially with small-footprint airborne lidar observations. Using an Area-Based Approach (ABA; Næsset, 2002), a series of grid-based metrics are produced (such as percentiles of point heights, or proportions of returns in different height strata) for a nominal grid resolution, corresponding to the inventory plot size. Many studies have used grid cells with an area of 400 m^2 (20 × 20 m) to match the extent of field-measured samples (i.e. circular plots, radius = 11.28 m; White et al., 2013). Grid cell size is also determined with reference to the local forest structural conditions, aiming to capture a set of trees that relates well to the structural characteristics present and minimizes error due to incomplete capture of large trees or edge effects (Frazer et al., 2011). From these statistical summaries of the point cloud data within the regularised grid, forest attributes are predicted. In a profiling context, returns from a portable laser profiler (PALS), which produces single lidar profiles along a flight line (Margolis et al., 2015; Nelson et al., 2009; Boudreau et al., 2008) can be used to develop models between individual profiles and field estimated AGB. Once predicted for the extent of the individual profiles, new models can be developed between these predictions and spatially comprehensive satellite data and ancillary information (e.g., terrain, climate), therefore allowing characterization of AGB over the broader landscape.

The most common lidar-derived forest attributes in the reviewed studies were height, volume, and AGB, either calculated using an ABA with airborne lidar metrics such as (Matasci et al., 2018a; Matasci et al., 2018b) and Luther et al. (2019) or modelled as a function of a waveform height, for example, Chi et al. (2015), who used ICESat GLAS profiles. Canopy cover and basal area were also commonly modelled followed by limited studies that extrapolated height complexity. (Fig. 1).

2.3. Predictor variables and area of analysis

In general, over three-quarters of the studies listed in Table 2 have extrapolated lidar-based metrics or lidar-derived forest attributes at scales of hundreds of thousands to millions of hectares, often defined as important ecological regions of interest (e.g., Canadian boreal, Brazilian amazon) or to apply to the total area of individual countries (such as China, Mexico or Chile). The broad extents over which forest structural estimates can be derived highlights the utility of the reviewed approaches and demonstrates a capacity for mapping over regional to global extents. The products generated are spatially explicit, applicable to all treed areas within a defined study region, and typically extend beyond the coverage feasible using airborne lidar data alone. The choice of geospatial predictors with which to extend lidar-based metrics or lidar-derived forest attributes across a landscape is a key methodological design decision. Studies have demonstrated the use of a wide range of predictor variables and often use spatial availability, cost, access, date of acquisition or development, and spatial resolution, as deciding factors for predictor incorporation. Below, we describe the three primary sources of predictor variables used in the studies: optical satellite data, RADAR data, and environmental data, specifically terrain and climate.

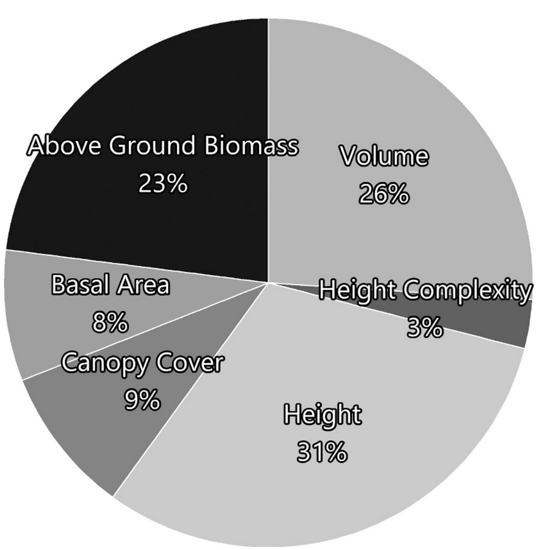

Fig. 1. Percentage of times various forest attributes are derived from lidar (from both air and spaceborne platforms) and subsequently extended over the landscape as captured by the reviewed studies of Table 2.

2.3.1. Optical satellite data

Of the studies reviewed (Table 2), one of the most common datasets used to extrapolate lidar-based metrics or lidar-derived forest attributes over large areas was optical imagery acquired from satellites; specifically the Landsat series of satellites. Landsat instruments have been acquiring multispectral data continuously from 1972 and since 1982 at 30-m spatial resolution (Goward et al., 2006). With the opening of the Landsat archive in 2008 (Wulder et al., 2012c), along with advances in high performance computing (Wulder and Coops, 2014), cloud masking (Zhu and Woodcock, 2014) and surface reflectance generation (Masek et al., 2006), land cover and condition characterization have become streamlined and more straightforward than previously possible (Magnussen et al., 2018). As a result, Landsat spectral bands, indices (e.g. Normalised Difference Vegetation Index (NDVI), Enhanced Vegetation Index (EVI)), as well as the tasseled cap transformation components (wetness, brightness, greenness), offer significant predictive capacity for extension over larger areas, particularly when finer scale forest structure predictions are needed.

Hudak et al. (2002) helped to pioneer the use of optical satellite imagery to extrapolate ALS observations over wide areas. Their study, which focused on managed forests of southwest Oregon, extrapolated small-footprint lidar estimates of canopy height using a single Landsat image acquired in 1999. The authors found that the Landsat shortwave infrared (SWIR) (ETM+, band 7) was the most useful predictor from a combination of raw bands and indices. Likewise, Badreldin and Sanchez-Azofeifa (2015) utilised a single Landsat scene to spatially extrapolate canopy height and AGB estimates in regenerating stands in Alberta, Canada. Results were then temporally extrapolated to selected annual Landsat images to examine changes in height and biomass between 1999 and 2011.

As availability of Landsat imagery continued to improve, studies began to incorporate multi-temporal Landsat images as predictors. The addition of temporal depth and change variables to the list of potential predictors has demonstrated improved modelling outcomes. Pascual et al. (2010), for example, utilised three Landsat summer images transformed using ratios and tasseled cap transformation over a two-year period to develop regression relationships with a lidar-derived canopy height model. They found SWIR-derived indices (wetness, Normalised Difference Moisture Index and Normalised Burn Ratio) to be the best predictors of height over pine forests in central Spain. Pitkänen and Käyhkö (2017) utilised NDVI derived from six Landsat images acquired in different summers as predictors to estimate the encroachment of trees into a semi-natural grassland mosaic in Finland. They found that high spatial resolution orthophotos outperformed Landsat imagery with the Landsat data having a relatively minor contribution for prediction, recognising that any temporal trend in grassland growth would benefit from denser temporal resolution satellite data. Beyond using a small number of dates, more recent studies have taken advantage of full time series Landsat reflectance to extrapolate across multiple years, capitalising on the fact that time series reflectance data is better at explaining variability in forest attributes than single year data (Pflugmacher et al., 2012). Bolton et al. (2018) and Matasci et al. (2018a), for example, used 30- and 33-year time series of annual Landsat best-available-pixel (BAP) composite images (White et al., 2014) and their associated disturbance history generated using the Composite-to-Change (C2C) approach

(Hermosilla et al., 2017; Hermosilla et al., 2016). Bolton et al. (2018) found that Landsat time series variables (such as 30-year spectral trend data) were important predictors in areas that had been recently disturbed such as forested sites experiencing fire or harvest. In these areas, extension of lidar-derived attributes such as volume were over-estimated in the absence of time series predictors. Bolton et al. (2018) also found that increasing the length of the time series to the full 30 years of the Landsat 30-m record improved accuracy compared to single year imagery. Further research by Bolton et al. (2020) demonstrated that a single optimal time series length is not necessarily determined by data availability (i.e., 30 years versus 10 years) and should be assessed on a case by case basis. The authors mention, however, that longer time series of Landsat data (>15 years) consistently produced more accurate estimates of forest attributes across Canada in a number of nationally-representative ecosystems. These improvements were attributed to the fact that single date Landsat imagery predictors in closed canopy stands are likely less sensitive to structural differences due to spectral saturation than predictor variables that incorporate long term spectral information.

Compared to Landsat, imagery from the Sentinel2 Multi Spectral Instrument (MSI) provides higher spatial resolution from 10 to 20 m and additional spectral bands (including bands focused on the red edge), which could help improve the model accuracies. Luther et al. (2019) utilised four mosaicked Sentinel2 scenes and derived predictor variables from the 10-m and 20-m spatial resolution bands to extrapolate lidar-based predictions of height, basal area, volume and AGB and found that extrapolation using the lidar-derived attributes decreased prediction errors by 8–28% compared with models developed directly from ground plots using a standard model-based inference approach. Li et al. (2015) utilised spectral and textural metrics from a single SPOT-6 image at 6-m multispectral, and 1.5-m panchromatic, spatial resolution to extrapolate lidar-derived canopy cover and AGB with relative RMSEs < 16.5% for a temperate forest in northwest China.

At a broader spatial scale, Moderate Resolution Imaging Spectroradiometer (MODIS) imagery has also been used effectively for extrapolating both lidar metrics and lidar-derived forest attributes for broader scale mapping and monitoring purposes. The broader spatial resolution of the MODIS spectral bands facilitates the use of these data for more regional and global scales. Lefsky (2010) notably extrapolated GLAS-derived vegetation heights using MODIS data that was spatially segmented using an object-based classifier with land cover. Lorey's height estimates were then extrapolated globally over all forested segments with a grid cell size of 500 m. Simard et al. (2011) used the Random Forests (RF) regression tree algorithm to extrapolate GLAS-based height estimates using seven globally-available predictors including climate, elevation, MODIS-based percent tree cover, and protection status to produce a 30 arc *sec* global height product. Chi et al. (2015) utilised MODIS 16 day, 500-m spatial resolution reflectance data products for 2006 as well as spectral indices and MODIS vegetation continuous field (VCF) and land cover data (that were later analysed using a principal component analysis) to extrapolate GLAS-derived AGB estimates across China in a number of regional ecozones. The authors concluded that the MODIS image data were useful for scaling up forest AGB from plots to subcontinental scales. At the national level, they found RMSE of less than 20% for over 50% of the forested provinces in China depending on their location and the amount of forest.

2.3.2. Radar

Synthetic Aperture Radar (SAR) and Interferometric SAR (InSAR) have also been used to extrapolate lidar-derived attributes. Both of these active remote sensing technologies have been useful for mapping biomass and forest structure depending on wavelength, particularly in areas that historically have lacked observations due to persistent cloud cover. In terms of SAR data, L band SAR is the most commonly used in these studies and is available as a global coverage from the Phased Array type L band Synthetic Aperture Radar (*PALSAR*) system onboard the Japanese Advanced Land Observing satellite (ALOS). L band SAR, with its longer wavelength, has been shown to be more sensitive to changes in biomass (Coops, 2002), especially at higher amounts of biomass, than the shorter wavelength C band SAR data more commonly available from RADARSAT, ERS1 and Sentinel1. X band RADAR has also been used, acquired from the Tandem X mission, which provides elevation information as well as insights into the amount (and height) of forest vegetation when compared to conventionally derived digital elevation models (Hyde et al., 2006). With moderate resolution pixel sizes, most of these SAR datasets offer complementary data to optical sensor as predictors for extrapolation.

As part of a simulation experiment for the proposed DESDynI (Deformation, Ecosystem Structure, and Dynamics of Ice) mission, Sun et al. (2011) modelled AGB over a 10 km^2 area as a function of lidar-based metrics describing the 50th and 75th height of returned energy from LVIS data. These data were then regressed to extrapolate the predicted AGB to PALSAR backscatter data acquired in 2007 with a spatial resolution between 3.5 and 9 m. All four SAR polarizations as well as total power of the SAR images, and coherence, were used to extrapolate the attributes derived from LVIS data. Results suggested that the multi channel SAR data explained more than 70% of the variation of the AGB information contained in the LVIS estimates. Similarly Li et al. (2016) utilised ALS data and PALSAR backscatter from a single image acquired in 2008 and texture variables over the Dayekou area, in Northwest China. Two combined products, namely backscatter ratio (Ratio) and difference (Diff), were generated based on the dual polarization PALSAR backscatter. From these products, AGB was predicted with an $R^2 = 0.62$ and an RMSE of 32 Mg/ha.

Kellndorfer et al. (2010) utilised the difference between Shuttle Radar Topography Mission (SRTM) derived ground elevation and conventional topographic mapping terrain models to derive the scattering phase center height, which has been shown to be correlated with the amount of vegetation present. Using this residual layer as well as slope and aspect information from terrain models, they segmented the residual images spatially over the entire area and then populated the segments with LVIS-derived heights. Montesano et al. (2013) utilised UAV-based L Band SAR and optical imagery to extrapolate LVIS estimates of AGB (as estimated by LVIS height) over a forest area in the eastern US. The combination of SAR and optical data proved to be the best model to predict AGB over the latter area. Cartus et al. (2012) utilised multi temporal ALOS PALSAR intensities and coherence as well as Landsat imagery to extrapolate stand level canopy height and growing stock volume across selected forest plantations in Chile. In total, 24 RADAR and 3 Landsat images were utilised. The HV polarization was found to be the most important predictor in the prediction depending on acquisition date. Validation indicated that over 80% of the variance was explained for LVIS extrapolated height across the plantations.

Lastly, Hyde et al. (2006) utilised LVIS canopy heights over the Sierra Nevada's in the United States and utilised a combination of Landsat with additional high spatial resolution optical texture metrics (QuickBird) and SAR combinations as predictors. Results indicated that complementary datasets (e.g. passive and active) produced more accurate predictions than single sensors alone, highlighting the potential importance of using combined predictor variables rather than relying on one dataset for the extension of the LVIS heights.

2.3.3. Terrain and climate

Terrain information has also been used widely for the extension of lidar-based metrics or lidar-derived attributes, recognising that variations in terrain can be a driver for changes in local meteorology, water access, and in turn, vegetation growth and structure. Globally, the increased use of the Advanced Spaceborne Thermal Emission and Reflection Radiometer (ASTER) digital elevation model (GDEM V2) is evident, allowing the generation of terrain related predictors such as elevation, slope, aspect, terrain wetness and solar radiation transformations. Bolton et al. (2018) and Matasci et al. (2018a) both found that elevation was one of the most significant variables in the prediction models, supporting the use of terrain related predictors. This is likely to be the case when the larger area covers elevation gradients resulting in changes in forest type or productivity (Bolton et al., 2018). In addition to terrain variables, Simard et al. (2011) in their global extrapolation of ICESat GLAS observations, utilised a number of climatic layers including precipitation, temperature, and seasonality, recognising the role climatic factors play on vegetation structure and growth at broad spatial scales.

2.4. Statistical approaches

Approaches to build relationships between lidar-based response variables and the satellite or ancillary predictor variables range in complexity, computing power requirements, data needs, and philosophies. Approaches can generally be divided into two categories: parametric and non-parametric. The former generally includes statistical regression methods, such as stepwise regression, geographically-weighted regression (GWR), and generalised linear models. In many cases however, the assumptions associated with the parametric approaches are not met with the data inputs commonly used in the modelling of lidar attributes, and predictors may include both categorical and continuous predictors. As a result, non-parametric approaches, including machine learning methods such as decision trees and RF, and imputation in the form of nearest neighbour (NN) have emerged as common approaches to obtain spatially-exhaustive estimates, as shown in Table 2. Both parametric and non-parametric approaches have advantages and disadvantages associated with them, as detailed in White et al. (2017) and as described below.

2.4.1. Regression

Pascual et al. (2010) utilised regression-based methods to build relationships between point cloud derived canopy height and a range of predictor variables with proportion of explained variance (R^2) from 0.15 to 0.70 depending on the predictor variables used. The authors flagged concerns associated with applying regression-based approaches including issues with residuals. The high number of potential predictors in their case was dealt with by utilising principal component analysis to reduce the dimensionality of Landsat spectral bands and ratios. Sun et al. (2011) also utilised regression-based approaches to model LVIS-derived AGB with SAR backscatter at 75-m spatial resolution. R^2 was over 0.70 using regression, and with other combinations of LVIS height metrics explaining up to 77% of the variance in AGB. . Despite their common use, regression models carry assumptions regarding data distributions, variance structures, and the independence of observations that are challenging to meet with many predictor data sets. Hudak et al. (2002) highlighted consistent estimation bias when applying regression approaches with respect to height by overestimating short stands and underestimating taller stands, indicating the tendency to underestimate the slope of a regression line if there is unmeasured variability associated with independent variables.

2.4.2. Imputation

One non-parametric approach to building models to relate lidar-based and lidar-derived attributes to predictor variables is through NN imputation. NN imputation methods are common when modelling forest plot inventory data as shown by Makela and Pekkarinen (2004), Tomppo et al. (2008) and Beaudoin et al. (2014), and are generally applied to fill data gaps found in the predictors (Zald et al., 2016). While regression-based methods predict new attributes that are missing, imputation “fills” in missing data by substituting values from common observations. A key attraction of imputation is that it is multivariate, non-parametric, and distribution free (Eskelson et al., 2009), seeking the single most representative plot whose values are to be imputed at a given location. One of the key advantages of the using NN is the ability to predict multiple attributes simultaneously. The search criteria to establish the best neighbour can be undertaken in a number of ways and can utilise an array of similarity measures (Hudak et al., 2008). Once the nearest neighbour is located, the training sample identifier is returned and its response variables assigned to the new sample to be predicted. One of the main characteristics of imputation is the preservation of the covariance structure among the response variables when the selected neighbour is one (Matasci et al., 2018b) as there is no averaging of the data in the prediction, rather original observations are reallocated over the extrapolation surface. However, there are trade offs in terms of accuracy and values of the selected number of neighbours (Eskelson et al., 2009).

Selection of predictors for use in imputation is particularly important, since these predictors are required to potentially characterize a suite of attributes, as well as being used for selection of the best neighbour (White et al., 2017). One approach to variable selection is that of Zald et al. (2016), whereby ALS metrics were used as response variables for the imputation, with derived attributes such as biomass and volume being transferred passively as auxiliary data. In this scenario, predictor variables were thus selected to characterize variability in the selected lidar metrics used as response variables. Packalén et al. (2012) summarise various methods available for selecting appropriate predictors for imputation. Another key consideration for imputation is the representativeness of the response data. In the context considered herein, it is the representativeness of the lidar plot samples used for the spatially-exhaustive predictions. These lidar plots must represent the full range of variability in forest structure (or the attribute of interest) on the landscape, because imputation cannot extrapolate beyond the range of values found in the response variables and will be prone to either under or overestimation if the response data is not sufficiently representative.

Bolton et al. (2018) applied a NN imputation method to extrapolate a range of lidar-derived attributes across 3500 km^2 of interior forest in British Columbia, Canada, using Landsat time series metrics. They found that Landsat imputed attributes correlated strongly with lidar-based estimates with R^2 values of 62 to 75%. Matasci et al. (2018a) also utilised a NN method to map a range of lidar-based metrics and lidar-derived forest attributes across the 5.5 M km^2 boreal forest of Canada. Lidar-based metrics and derived attributes were extracted from >25,000-km of transects collected across the boreal, and NN was used to extrapolate 10 forest structural attributes. Validation of the models indicated explained variance between 49 and 61% for the key variables such as canopy cover, stand height, basal area, stem volume, and AGB. Additionally, elevation, and geographic coordinates were key sources of information in the imputation.

2.4.3. Machine learning

The appeal of machine learning approaches in ecology has grown significantly in the past decade due to an increase in open access data, software tools, and computing power. In these approaches, datasets are mined efficiently by algorithms, which seek to build rules and decisions to model the required attribute. Decision trees and RF methods are common in ecology due to key features including an ability to deal with collinear datasets, to exclude insignificant variables, and to allow for asymmetrical distribution of samples (De’ath, 2002). Pitkänen and Käyhkö (2017) utilised RF methods to develop models between ALS attributes and Landsat predictors over grassland in Finland on the assumption that RF had a low tendency to overfit, was simple to implement with few parameters, was efficient to run with large datasets, and results were easily evaluated using error rates and measures of variable importance. They predicted three classes of grassland/woodland condition with a categorical model output and classification accuracies of over 90%. Kellndorfer et al. (2010) implemented a RF approach to impute LVIS height using SRTM residuals over a forest area in the Eastern US. Results indicated that validation using forest plot information outside the LVIS profiles was successful, with the proportion of explained variance >0.70 and an RMSE of 13% of maximum height. Luther et al. (2019) compared RF and regression methods for extrapolating lidar-derived predictions of height, basal area, volume and AGB using a combination of optical, RADAR and terrain predictor variables and found that RF models performed significantly better than regression models for extrapolating all attributes ($p < 0.05$). Additionally, the RF predictions using model-based inference with hierarchical modelling resulted in decreased prediction errors of 8–28% when compared with standard model-based inference linking the spatially-exhaustive observations directly with ground-based field data. As RF model frameworks have become more common, so too has the variety of methods to compute the distance of similarity metric within the NN approaches. As shown in Table 2, more recent studies utilise a NN imputation framework with a RF-estimated distance metric. In these cases, the RF-based kNN imputation is based on a non-euclidean distance measure derived by running a target observation through RF models trained from reference observations. The proximity of a target to a reference observation is then assessed by calculating the proportion of RF trees where they share the same final node (Crookston and Finley, 2008). In the case of multiple response variables, RF models are built for each response variables but proximity measures are combined in order to find the k most similar observations considering all response variables simultaneously. RF-based NN imputation is therefore a multivariate approach, which also has the advantages of being non-parametric and able to handle both continuous and categorical response variables (Crookston and Finley, 2008; Eskelson et al., 2009; Queinnec et al., 2020).

2.4.4. Geospatial statistics

Exploiting the inherent spatial nature of lidar-derived attributes and predictors can provide additional insights and strengths into developed relationships. Geostatistical approaches, such as kriging methods, provide techniques to interpolate observations over the landscape using a mathematical model that incorporates spatial variance into the overall spatial variance in a dataset (Webster, 1985). Ordinary kriging, the most common form (Krige, 1966), is a spatial modelling technique that provides optimal and unbiased estimates of unknown values from sample data (Curran and Atkinson, 1998). Cokriging extends ordinary krigging to account for more predictors and is more common when one variable (i.e. AGB) is under sampled compared to spatially-exhaustive predictors. In co-kriging, the predictor variable is calculated using the autocorrelation of the primary variable; however, co-kriging also exploits the cross-correlation of the primary and secondary variables (Tsui et al., 2013). Lastly, regression kriging is a hybrid approach that combines a regression model with kriging of the regression residuals (Goovaerts, 1997). Hudak et al. (2002) evaluated five spatial and a-spatial methods to integrate ALS and Landsat ETM datasets and provided unique insights into the most appropriate methods that should be applied with this type of data for estimating and mapping forest canopy height. Results suggest that the kriging and co-kriging approaches produced less biased results than regression, and that co-kriging methods were preferable as they preserved vegetation patterns akin to regression, yet improved upon estimation accuracies from regression models alone. Li et al. (2015) examined two types of kriging to estimate lidar-derived canopy cover and AGB. They found that regression kriging showed the least error for both ALS attributes with RMSE values of 11.2% and 17.3%, respectively. The observed spatial patterns after the interpolation exhibited more consistent variation compared to simple regression. In general the regression kriging was superior because it preserved spatial patterns and improved global and local estimation accuracy.

2.5. Accuracy assessment approaches

Once the extension of the attributes over the landscape has been undertaken, a critical step is to assess the correspondence between what was predicted and what was observed (Miller et al., 2004). Authors highlight difficulty in obtaining suitable accuracy assessment data with which to independently assess the accuracy of the predictions. This is partly because of the complexity of the processes impacting the error budget in final outputs. Generally, assessment of the accuracy of the models should be undertaken using data not used in formulating the original lidar-based prediction models or the spatially-exhaustive models. However, forest plot data with which to validate models are often in short supply and as a result are then utilised in the model development rather than segregated for independent model validation in order to explain the most variance and hence build the best models with the available data. An assumption that any lidar-based or lidar-derived forest attribute is estimated without error is the main shortcoming in many of these approaches. Thus, although lidar-based and lidar-derived predictions are assumed to be error free, this is known not to be the case. There are biases associated with the acquisition parameters (e.g., aircraft altitude and speed, sensor, scan angle and frequency, flight line overlap) of small-footprint lidar data and lidar sampling procedures associated with the large-footprint waveform data. Moreover, canopy architecture (deciduous vs coniferous, high and low canopy cover, stand heterogeneity) is also known to influence the biases observed in lidar observations of height, as well as time of year (leaf-on vs leaf-off conditions). Neigh et al. (2013) also discuss potential errors associated with allometry, which is often used to derive estimates of volume and biomass (Réjou-Méchain et al., 2019), and geolocation error between ground plots and lidar observations (Frazer et al., 2011). In the case of lidar-derived forest attributes, regression is most commonly used to link lidar metrics to forest attributes producing accuracy estimates as shown by White et al. (2013); however, there is little consensus of what is a sufficiently-accurate model to warrant applying over broader areas. Metrics that explain the limits of agreement (LoA; Bland and Altman, 1986) have also been proposed as more appropriate indicators of success, in addition to standard regression-based accuracies. Extrapolating these lidar-based or lidar-derived estimates to the broader area also introduces biases and errors in the resulting predictions making accuracy assessment difficult. It has been clearly demonstrated that when forest attributes are derived from lidar metrics using an ABA approach, the variance of the final estimate is underestimated when the predictions are used as observed data (Saarela et al., 2016; Holm et al., 2017; Urbazaev et al., 2018).

As highlighted in Table 2, only half of the studies used independent information on forest attributes to verify the prediction results. While use of independent validation data is the ideal scenario, these accuracy estimates may also be biased, depending on the location, and the number and age of the data being used to independently validate the spatially-exhaustive predictions. In addition to independent error assessment, a number of studies have quantified the propagation of error through the process. Saarela et al. (2016) proposed a new estimator accounting for the uncertainty of the intermediate model when ordinary least square regression models are developed for both the forest attribute estimation and its extrapolation. When modelling is undertaken using machine learning approaches, accuracy is commonly assessed with cross validation, by dividing the dataset into a series of subsets and then repeating the model development phase on a limited set of subsets, testing the accuracy of the model on the remaining subsets. This process is repeated a number of times, randomly drawing samples within each subset. This produces multiple assessments of the model error that can then be averaged to produce overall model performance statistics. Imputation-based approaches produce complex error structures; however, the widespread use of these approaches has resulted in the formulation of uncertainty using recently-developed variance estimators for imputation predictions (McRoberts et al., 2018). These variance estimators require significant computation resources to compute and may be limiting when extrapolating over large areas (Zald et al., 2016). Although a number of the aforementioned studies (e.g., Kangas, 1999; Frazer et al., 2011; Melo et al., 2018; Wang et al., 2019) provide some form of accuracy assessment, either through leave-one-out cross-validation or out of bag errors, independent validation or averaging predicted attributes over larger areas and making comparisons with other sources of available reporting statistics (e.g., jurisdictional reporting statistics), less effort has been expended to analyze the sources of error and account for how they propagate to the overall uncertainty of the extrapolated product. Uncertainty estimation of broad area predictions is not straightforward, namely due to the random variation that arises from multiple sources of error: the field observations, the sampling, and the model (Phillips et al., 2000; Melo et al., 2018). Quantifying these errors through error propagation can provide insights into those sources of error that need to be addressed in order to minimize the uncertainty of the final predictions.

An alternate accuracy assessment approach was presented by Holm et al. (2017). Instead of developing models to extend predictions from an initial lidar-based forest attribute model, the authors predict the lidar-based metrics that are used in the first modelling step as functions of the broader coverage variables. For example, models were developed to predict the 95th percentile of return heights and the proportion of returns above 2 m, and both attributes were used in the models to predict biomass directly with lidar. Holm et al. (2017) showed that this approach resulted in all of the initial lidar point cloud and spatially-exhaustive variables being considered in the same equation and therefore all of the variances and covariances of both models can be taken into account. The authors demonstrate that inclusion of the lidar-based prediction model error is significant and important, and when this error is explicitly accounted for in the modelling, the final model's standard error increased four times compared to ignoring the first stage model error. With respect to model error calculations, Saarela et al. (2016) and Holm et al. (2017) both received the same estimates and model variances if they use the same list of predictor variables in the two models that relate the 3rd-2nd phase (e.g., ground-ALS) and 2nd-1st phase (e.g., ALS-satellite) (Holm et al., 2017). Both of these approaches are available in an existing R package available for download (Saarela et al., 2020a). Urbazaev et al. (2018) demonstrated a method for estimating the uncertainties at the pixel level using Monte Carlo simulations, estimating the total error in the final estimate of AGB by repeating the modelling steps 100 times, starting with a set of 100 field-estimated AGB values that included a randomly distributed error.

For the review of studies in Table 2, when accuracies are reported it is most often as the coefficient of determination (R^2), which is the proportion of variance explained by the model produced using regression methods. Mean error (ME), mean absolute error (MAE), and Root Mean Square Error (RMSE) in either absolute units or as proportions of the mean response (observed) value (RMSE%) are also often provided when independent validation is used to quantity the degree of correspondence between the observed vs predicted values.

Fig. 2 provides a summary of the reported accuracies of the reviewed studies in Table 2. Height and AGB are the most common attributes extended across large areas, and these attributes also have the widest range in accuracies. The variance explained in predictions of forest height ranged from $R^2 = 0.38$ to 0.90, whereas for volume, R^2 ranged from 0.1 to 0.7 and AGB R^2 ranged from 0.35 to 0.78. In contrast, basal area and cover, while less common, are more consistent in their accuracies with R^2 ranging from 0.64 to 0.66 and 0.77 to 0.88, respectively. For RMSE, height errors ranged from 2 to 6 m, volume errors ranged from 60 to 87 m^3/ha and biomass error was between 28 and 44 Mg/ha. RMSE% ranged from 12 to 34% for height, 22 to 34% for volume and 23 to 29% for basal area.

In recognising that accuracy assessment can be challenging, a number of authors examined the predicted broad scale patterns and assessed the magnitude of predictions by comparing results with other publicly-available datasets, rather than providing an independent validation. For example, Chi et al. (2015) compared the models of AGB aspatially across a number of Chinese forest-dominated provinces. This allowed AGB estimates to be rolled up to province-wide estimates and then compared to national reporting statistics.

3. Current trends in modelling studies

3.1. New lidar-based response and predictor variables

In recent years we have seen rapidly increasing in both spatial coverage, and point density aircraft-based small-footprint datasets. Recent technological advances for example have led to the development of single photon sensitive detectors. While typical discrete or full-waveform airborne instruments require hundreds to thousands of photons to trigger a return, single-photon sensors can detect individual backscattered photons and lower energy pulses, and can be operated at higher altitudes (Degnan, 2016; Swatantran et al., 2016). Single-photon lidar (SPL), for example, uses a very short pulse of green (532 nm) laser light that is split into a 10 × 10 grid of beamlets with a diffractive optical element (Degnan, 2016). Each beamlet has a low divergence of 0.08 mrad that results in non-overlapping footprints on the ground and is received by an individual detector aligned along its path (Mandlburger et al., 2019). The system configuration allows an increase in both areal coverage and point density and a reduction in flying time and associated costs compared to conventional airborne small-footprint systems (Swatantran et al., 2016). The instrument is inherently sensitive to background solar noise when operated in daylight conditions, which requires subsequent noise filtering steps that could affect the accuracy of data. Moreover, the conventional intensity measure of the returns, which can be used for tree species characterization, cannot be derived similarly from single photon detection events. SPL still provides a proxy for intensity based on the cumulative count of detected photons although its range is limited (Hartzell et al., 2018). Nevertheless, heightened point densities of single photon lidar could enable the extraction of new types

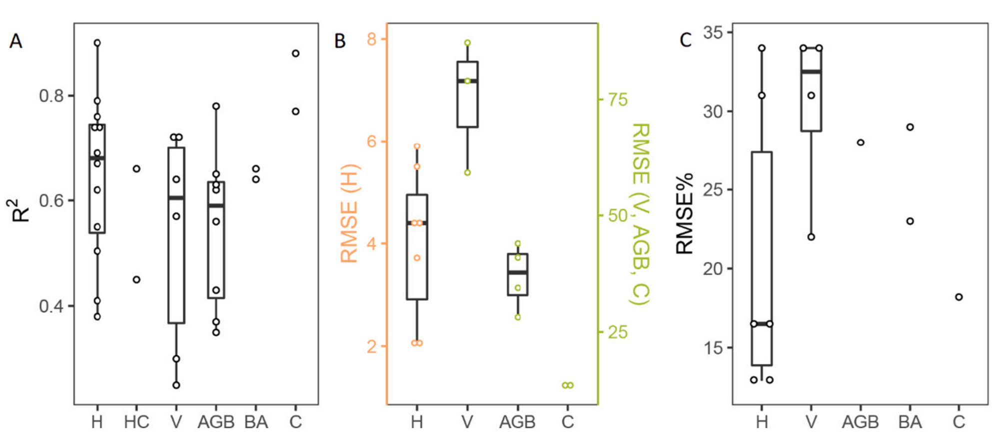

Fig. 2. Distribution of a) R^2, b) RMSE, and c) RMSE% of the extended forest attribute predictions (H: height, HC: height complexity, V: volume, AGB: aboveground biomass, BA: basal area, C: canopy cover) for the studies reported in Table 2.

of point cloud metrics and the estimation of new forest attributes (Wästlund et al., 2018).

In 2019, two new satellite missions began to release data to the scientific community, significantly improving the availability of satellite lidar observations at global or near global scales. In 2018, NASA launched ICESat-2, a laser altimeter satellite designed to quantify ice sheet contributions to sea level change (Markus et al., 2017). While the key mission of ICESat-2 is ice-related, the laser altimeter also operates over land allowing a number of geophysical products to be extracted including information on aboveground vegetation (Neuenschwander and Pitts, 2019). The sampling nature of ICESat-2 should allow determination of global vegetation height at an equatorial spacing of less than 2 km over a two-year period (Markus et al., 2017). The Advanced Topographic Laser Altimeter System (ATLAS) instrument onboard ICESat-2 had a nominal design footprint size of 17 m in diameter (Neuenschwander and Pitts, 2019); however, a smaller footprint size has been realized in ATLAS operation (11 m in diameter; Neuenschwander et al., 2020). As the ATLAS laser operates in the green wavelengths of the electromagnetic spectrum (532 nm), the data can be noisy due to solar contamination and effective noise filtering algorithms are necessary (Neumann et al., 2019). The ATL08 data product provides a number of canopy height percentiles (from 25th to 95th) for 100-m long segments, with each backscattered photon labelled as either noise, ground, canopy or top of canopy (Neuenschwander and Pitts, 2019). A gridded data product of canopy height, cover and ground elevation is also planned to be delivered annually at a coarse spatial resolution (500 m to 1 km) towards the end of the mission, which is intended for use in global studies and broad characterisations of forest structure.

The second spaceborne instrument that is providing near global coverage of lidar footprints is GEDI (Dubayah et al., 2020). GEDI is a full-waveform lidar instrument on the International Space Station with three active 1064 nm lasers that combined produce 8 tracks of data with a ~ 25-m footprint. The system uses a 4.2-km swath width within which each of the 8 tracks are separated by 600 m (Dubayah et al., 2020). Unlike ATLAS, GEDI is specifically designed to measure forest structure, with the goal of producing mean AGB estimates and a range of other canopy attributes such as canopy height and foliage profiles between 51.6° N and S latitudes over forested regions (Patterson et al., 2019). The GEDI lidar footprints are 25-m wide, spaced 60 m apart along a ground track and after two years will have covered the majority of 1-km cells with two or more ground tracks with efforts underway to produce both broad-scale gridded products as well as fine spatial scale products through modelling with, for example, Landsat imagery.

Opportunities exist for these spaceborne lidar systems to provide datasets suitable as predictor variables. Given that the relationships between airborne lidar measurements and these spaceborne observations are likely to be stronger than with optical or other satellite active remote sensing spatially-exhaustive predictors, there is significant potential in using these regional or global summaries to provide improved predictions of lidar-derived attributes across large areas, especially in broader scale monitoring applications. Moreover the use of these spatially-exhaustive, three-dimensional predictor variables in concert with optical time series could be very useful, allowing model calibration, product validation, and unique modelling opportunities using the independent structural estimates.

3.2. Advances in modelling approaches

A number of algorithmic advances may help in the extension of lidar-based metrics and forest attributes across large areas. Often, the goal of extension is to predict several attributes concurrently, and to ensure that those attributes remain logically consistent (Zald et al., 2016). Conventionally, a set of predictors are input into the extension method and an attribute is modelled using the predictors. If the aim is to predict a single target attribute (such as AGB), then it is known as a single target prediction task. Many of the studies reviewed used this approach and predicted a single attribute, commonly height or AGB (Table 2). In cases where several target attributes are predicted simultaneously with one model, it is known as a multi-target prediction task. Imputation is one approach that facilitates multi-target prediction, as it allows a suite of forest attributes to be transferred to a new location. Bolton et al. (2018) and Matasci et al. (2018b) both used a RF NN imputation method as demonstrated by Crookston and Finley (2008) where RF proximity matrices are built for each response variable and the nearest neighbour is the observation that best fits all the response variables at the same time. Another approach that can be used to estimate several dependent variables in a single step is Seemingly Unrelated Regression (SUR) (Greene, 1993; Penner et al., 2013). New algorithmic developments include multi-target regression trees allowing for the generation of several target attributes simultaneously, where terminal nodes or leaves of each regression tree are stored as vectors rather than individual values. Multi-target regression could ensure that extrapolated canopy cover is consistent with volume over the same forest type (Kocev et al., 2009).

As satellite-based lidar observations become more widespread, gridded global and near-global datasets of derived forest attributes will become more common place. We note that the grid resolution of ultimate products will be more spatially coarse than the lidar data footprint. This increase in availability and coverage of spaceborne lidar measures will likely bring two complementary approaches to extending lidar observations at these broad scales. Firstly, from the satellite-based perspective, lidar-based metrics and lidar-derived forest attributes will be strongly linked to height measurements especially in the case of ICESat-2. Estimates of height will then drive global estimate of forest attributes of interest such as biomass and carbon. Secondly, in the case of extension of small-footprint lidar point clouds acquired from aircraft, the ability to derive a range of forest attributes within target cells, will also allow other attributes to be derived beyond height and biomass and include attributes such as volume, basal area and diameter.

3.3. Assessing change in forest attributes over time

Perhaps one of the most important uses of extended layers of forest attributes is for assessing change in forest structure over time. Most studies reviewed extended attributes at a single point in time, providing spatially-exhaustive estimates for key attributes for a single time period. In reality, however, many agencies would like to be able to track estimates of attributes like AGB over time to inform on REDD+ activities and other national level reporting obligations (Wulder et al., 2020). Matasci et al. (2018b) was one of the few studies that extended ALS attributes across time by utilising temporal metrics from the Landsat record to drive the models. In addition to single image dates from Landsat spectral data, Matasci et al. (2018b) utilised spatially-exhaustive predictors such as time since most recent disturbance, which varied on an annual basis. These predictors allowed AGB and other attributes to be modelled annually over a 30-year period. These models allow imputation across the natural growth sequence of a forest stand and they allow canopy structure and height to be explicitly modelled as stands age. Badreldin and Sanchez-Azofeifa (2015) had similar aims assessing change in AGB over time at a previously disturbed site in western Canada. They predicted biomass at 5-year intervals using a regression-based approach and Landsat predictors acquired at different times. Changes in AGB were then assessed by differencing the 5-year predictions to document how biomass recovered following disturbance.

Recently, Wulder et al. (2020) utilised annual predictions of lidar-derived aboveground biomass to quantify biomass dynamics, partitioned by disturbance over the forested ecosystem of Canada. By utilising extension models in a temporal analysis, they were able to account for changes in biomass as a function of disturbance dynamics, demonstrating that biomass consequences associated with disturbance are highly dependant on the type of disturbance occurring over the forested landscapes. Biomass changes (both positive and negative) were quantified by disturbance type, with post disturbance recovery of biomass also documented. Extrapolating biomass to the same spatial grain as Landsat enables a direct link to other Landsat-derived spatial datasets representing the same scale (including land cover and change datasets).

Næsset et al. (2013) developed methods to report biomass change over an 11-year period, with attribution by a range of activities representing deforestation and degradation, using airborne lidar and stratified ground-plot data in both a wall-to-wall and sample-based approach. Extension of forest attributes can also be used to characterize sudden changes such as burns caused by wildfires. Garcia et al. (2017) quantified losses in AGB from the California Rim fire in 2013 by extrapolating post-fire lidar-derived AGB estimates using both pre-fire and post-fire Landsat imagery. Using support vector regression models for the modelling, they report a R^2 of 0.72 and 0.60 and relative RMSE of 41.94% and 50.15% for pre-fire and post-fire estimates of AGB assessed on an independent validation set.

3.4. *Continued importance of ground plot measurements to support lidar extension efforts*

As highlighted throughout this review, field measurements of forest attributes are critical in any modelling endeavor. Although it may seem incongruous that with a profusion of airborne and spaceborne lidar datasets providing accurate characterizations of forest structure, there is a continued need for quality ground plot data to develop predictive models and to verify lidar-based predictions. While our understanding concerning the number (Strunk et al., 2014), distribution (Hawbaker et al., 2009), and transferability (Fekety et al., 2015; Tompalski et al., 2019) of ground plots to support lidar-based estimates continues to evolve, some form of ground measurement is nevertheless required, either to support local model calibration or to provide independent validation. Moreover, it is imperative that these ground plots represent a fixed area and are acquired with a high level of geospatial precision and accuracy (White et al., 2013). Positional accuracy is critical, as airborne lidar systems have very low positional errors (well less than 1.0 m) and satellite-based lidar systems also produce very accurate spatial datasets (between 5.0 m for ICESat-2 to 10 m for GEDI (Neuenschwander and Magruder, 2019; Dubayah et al., 2020, respectively). As part of their objectives, spaceborne missions such as GEDI have explicitly included the development of ground plot databases with which to calibrate, test, and improve models of key forest attributes of interest. The GEDI Forest Structure and Biomass Database (FSBD) (Duncanson et al., 2020), encompassing measurements from over 1 million trees in tropical and temperate vegetation types globally, is critical in providing confidence in near-global predictions of carbon and biomass change studies.

3.5. *Importance of open data*

Data policies continue to influence scientific applications and the pace of innovation and uptake of remote sensing technologies in forest applications (Wulder and Coops, 2014). Both ICESat-2 and GEDI missions have open data policies, with investments in ground segments that facilitate data sharing and access (Dubayah et al., 2020; Neuenschwander et al., 2020). Increasingly, national and jurisdictional lidar datasets are also openly accessible in some form or another (e.g., Kotivuori et al., 2016; Magnussen et al., 2018; Fradette et al., 2019), further expanding the opportunities to depend upon these data for large area applications and spatial extension of key forest attributes to unmanaged forests and/or areas where existing inventories are either non-existent or out of date (Bolton et al., 2018).

4. Outlook

Examination of the previous research detailed throughout this review provides the opportunity to highlight a number of emerging trends and directions identified and foreseen to facilitate the further linking of lidar metrics and lidar-derived forest attributes with varieties of spatially exhaustive geospatial data. We discuss a number of these anticipated future directions below, which cover inclusion of spatially-explicit layers that represent ecological processes, such as forest change, strategic efforts to standardize methodological approaches, increased access to high quality, open datasets to facilitate extension, and consensus towards best practices for validating and estimating uncertainty in the derived information products.

4.1. *Inclusion of ecological processes, time series, and disturbance at a relevant monitoring and reporting scale to enhance accuracy*

Across the studies reviewed, the need and requirements for spatially-exhaustive, lidar-based metrics or lidar-derived forest attributes differs depending on the ultimate application of the datasets. Some studies, for example, have estimated forest height and AGB globally for broad scale descriptive and monitoring purposes, whereas others have derived products at finer spatial scales to provide information for forest inventories and management. As noted, the bulk of the studies reviewed provide estimates at national or biome scales. As with other remote sensing informed studies, the derived information content is a function of the image characteristics and this is true of the wall-to-wall extension products as well. The spatial grain of derived products will replicate or be coarser than the source lidar data. Similarly, the spatial resolution of the satellite data used will typically drive the finest possible spatial grain for derived products from spatial modelling procedures (Coops et al., 2004). In turn, the information content of any derived products and the possible use is formed by these considerations. Given a goal to inform studies of ecological or economic importance, the ability to link anthropogenic activities to landscape change type (e.g. wildfire, harvest, non-stand replacing disturbances etcetera) and persistence of changes is increasingly required. For instance, forest change due to wildfire versus agricultural expansion have differing long term effects important for carbon monitoring. While initially coarse spatial resolution products played a key role in demonstrating the capacity for lidar-based modelling of forest heights and biomass, the meaning of an average height or biomass estimate representing a 500 m or greater grid cell is of limited utility and insensitive to meaningful or actionable monitoring, especially over heterogeneous ecosystems. Current capacity for finer spatial resolution depictions with increasing temporal regularity, such as Landsat-based studies, now offer opportunities for applications over large areas and at a spatial grain informative to management, reporting, science, and policy development.

4.2. *Standardization of modelling approaches to support extension*

As applications differ, so has the selected methodological approach, resulting in a proliferation of different statistical techniques. Some standardization around the most appropriate statistical methods to use for modelling as a function of both spatial scale of the prediction, and extent, would significantly benefit future efforts. For example imputation-based approaches have clear advantages when large numbers of samples are able to be extended over the landscape, and regression offers insights when predictions may extend beyond the observation range. As a result, guidance and best practices towards appropriate methods for extending attribute estimates given multiple objectives would be a worthwhile endeavor that could be achieved through synthesis papers, or benchmarking experiments similar to a study undertaken recently by Cosenza et al. (2020).

4.3. *Development of more, high quality, open datasets to facilitate modelling*

A wide variety of data sources have been used to extend lidar-based metrics or lidar-derived forest attributes. Key to generating spatially exhaustive predictions is the development of open access data policies and efficient platforms or mechanisms for sharing data. Older studies, especially at global scales, utilised MODIS imagery, in part, due to its availability and open access data policies. With the more recent opening of the Landsat archive and similar policies guiding access to data from the Sentinel series of satellites, there is significant added utility of using these moderate scale spatial resolution datasets to link with lidar metrics. Research into the most appropriate ways to link archival remotely sensed data, such as trends and spectral trajectories over time, or inclusion of forest cover change information will likely increase when extending lidar-derived metrics over time and space. We note that a number of studies utilised more specialized data sets that may not be readily or freely available. Cost and availability can be problematic in situations where standardized approaches are to be implemented in new locations.

4.4. Ongoing development of parametric and nonparametric modelling frameworks to include additional phases of sampling

While there has been significant development in statistical approaches to assist in the modelling parameterization over the past decade, these frameworks need to be continually developed to include additional phases of sampling. Specifically, one additional layer of error that is common throughout all of these studies, yet often ignored, is the initial allometric equations used to derive some of the forestry attributes. For example, calculations of volume are virtually always based on measurements of DBH and height and yet the error inherent in these allometric equations is often ignored. In recent work on this topic, Saarela et al. (2020b) found that up to 75% of the relative root mean square error in biomass prediction could be attributed to allometric model uncertainty. Importantly, they provide a hierarchical sampling framework which allows this error to be quantified and implications on overall model predictions to be assessed across broader spatial scales. Secondly, while these new frameworks have been designed around parametric solutions, the interest by the remote sensing community in nonparametric approaches for example, RF, could be the focus of additional model development given their widespread use by the community.

4.5. Establishment of best practices for validating and estimating uncertainty in the derived information products

In simple cases where lidar metrics are extended across the landscape, errors can be more easily determined. In situations where lidar-derived forest attributes are extended, the calculation of an error budget is much more complex and requires significant statistical knowledge (e.g., Saarela et al., 2016; Magnussen et al., 2018; Saarela et al., 2020b; Holm et al., 2017). Simply validating a prediction using independent field observations, whilst conceptually simple, is often difficult due to lack of available data, mismatches in temporal and spatial scales, and lack of an inability to cover the entire range of the predicted estimates, or the entire geographic area. Recent trends towards free and open reproducible software to allow users to more readily calculate error budgets should see error budgets produced more readily. The production of accessible best practice methods that allow the errors inherent in these predictions to be quantified as predictions move from plot to lidar estimations and ultimately spatial extension across for landscape is important. Recent initiatives such as the Committee of Earth Observation satellite (CEOS) Land Product Validation (LPV) subgroup have developed a Biomass Protocol promoting good practices for validation of the lidar mission satellite products and to ensure observed change from these missions are real and not a function of the errors accumulated through the modelling process. Similar emphasis should be focused on methods and statistical approaches of assessing error and estimating uncertainty. Recent missions, specifically ICESat-2 and GEDI on the ISS, will continue to provide sample-based datasets as their basic data product, which suggests that users will continue to be looking for approaches to extrapolate these estimate over broader spatial units. These missions will allow key technological issues to be resolved and should provide a framework and blueprint for continuing satellite-based lidar systems, focused on assessing forest structure and terrain.

5. Conclusion

Lidar data has become a key data source for predicting a range of forest attributes. However, with a few notable exceptions, coverage of airborne lidar is often constrained in both time and space, whereas spaceborne lidar has typically been sample based. Both situations necessitate statistical approaches to extrapolate these lidar observations or derived forest attribute estimates over larger areas, or through time. This review has demonstrated that this extension has been undertaken over a broad range of spatial scales, in order to produce attributes at the local or regional scale for forest management, as well as national- or global-level estimates to support scientific investigations and forest assessment and monitoring efforts. Common among the research examined herein is the derivation of key forest attributes such as height and volume that are valuable for finer scale forest management activities, as well as AGB, which is a critical indicator to assess the impacts of global climate change. Modelling approaches can be applied to meet both of these information needs, providing systematic, and consistent predictions that can overcome some of the conventional challenges associated with monitoring large areas, providing both spatial and attribute detail at a meaningful spatial grain that is informative of anthropogenic drivers of change. While applications and examples of approaches are increasingly common, the lack of standardized, spatially exhaustive open access datasets, as well as community consensus on methods and best practices limits the broader uptake and operationalization of these approaches. In particular, advancements could be made by the development of accessible statistical methods to assess error propagation from field plot predictions to final modelled attributes, as we see a greater need these types of methods given the increasing availability of spaceborne lidar systems.

Credit author statement

Manuscript was developed, written, edited and reviewed by all co-authors.

Declaration of Competing Interest

The authors declare that they have no known competing financial interests or personal relationships that could have appeared to influence the work reported in this paper.

Acknowledgements

This research was funded by the AWARE (Assessment of Wood Attributes using Remote Sensing) Natural Sciences and Engineering Research Council of Canada Collaborative Research and Development grant (crdpj 462973-14). Industrial Support was received by: FP-Innovations, West Fraser, Corner Brook Pulp and Paper, Ryam Lumber (formally Tembec), and JD Irving. Smaller contributions were received by Columbia Forest Products, and Hearst Forest Management. Significant in-kind support was provided by the Canadian Forest Service - Canadian Wood Fibre Centre (CWFC), Northern Hardwood Institute and Provincial Forestry Ministries. The universities involved in AWARE were The University of British Columbia, Laval University, University of New Brunswick, University of Sherbrooke, Queens University, University of Quebec at Montreal, University of Toronto, Nippissing University and Laval University. We are grateful to Veronika Gukova and Bryn Gerson for editorial help with this review. Two anonymous reviewers provided very thoughtful feedback on the initial drafts, and the manuscript is improved by their efforts. Thank you.

References

Abshire, J.B., Sun, X., Riris, H., Sirota, J.M., McGarry, J.F., Palm, D., Yi, D., Liiva, P., 2005. Geoscience laser altimeter system (GLAS) on the ICESat mission: on-orbit measurement performance. Geophys. Res. Lett. 32, L21S02.

Andersen, H.E., Strunk, J., Temesgen, H., Atwood, D., Winterberger, K., 2012. Using multilevel rmote sensing and ground data to estimate forest biomass resources in remote regions: a case study in the boreal forests of interior Alaska. J. Can. Remote Sens. 37, 596–611.

Badreldin, N., Sanchez-Azofeifa, A., 2015. Estimating forest biomass dynamics by integrating multi-temporal Landsat satellite images with ground and airborne LiDAR data in the coal valley mine, Alberta, Canada. Remote Sens. 7 (3), 2832–2849.

Beaudoin, A., Bernier, P.Y., Guindon, L., Villemaire, P., Guo, X.J., Stinson, G., Bergeron, T., Magnussen, S., Hall, R.J., 2014. Mapping attributes of Canada's forests at moderate resolution through k NN and MODIS imagery. Can. J. For. Res. 44, 521–532.

Blair, J.B., Rabine, D., Hofton, M., 1999. The laser vegetation imaging sensor (LVIS): a medium-altitude, digitization only, airborne laser altimeter for mapping vegetation and topography. ISPRS Photogram. Remote Sens. 54, 115–122.

Bland, J.M., Altman, D.G., 1986. Statistical methods for assessing agreement between two methods of clinical measurement. Lancet 327, 307–310.

Bolton, D.K., White, J.C., Wulder, M.A., Coops, N.C., Hermosilla, T., Yuan, X., 2018. Updating stand-level forest inventories using airborne laser scanning and Landsat time series data. Int. J. Appl. Earth Obs. Geoinf. 66, 174–183.

Bolton, D.K., Tompalski, P., Coops, N.C., White, J.C., Wulder, M.A., Hermosilla, T., Queinnec, M., Luther, J.E., van Lier, O., Fournier, R.A., Woods, M., Treitz, P., van Ewijk, K., Graham, G., Quist, L., 2020. Optimizing Landsat time series length for regional mapping of lidar-derived forest structure. Remote Sens. Environ. 239, 111645.

Boudreau, J., Nelson, R.F., Margolis, H.A., Beaudoin, A., Guindon, L., Kimes, D.S., 2008. Regional aboveground forest biomass using airborne and spaceborne LiDAR in Québec. Remote Sens. Environ. 112 (10), 3876–3890.

Brown, R., Hartzell, P., Glennie, C., 2020. Evaluation of SPL100 single photon Lidar data. Remote Sens. 12 (4), 722.

Cartus, O., Kellndorfer, J., Rombach, M., Walker, W., 2012. Mapping canopy height and growing stock volume using airborne Lidar, ALOS PALSAR and Landsat ETM. Remote Sens. 4 (11), 3320–3345.

Cassel, C.-M., Särndal, C.-E., Wretman, J.H., 1977. Foundations of inference in survey sampling. Wiley, New York.

Chi, H., Sun, G., Huang, J., Guo, Z., Ni, W., Fu, A., 2015. National forest aboveground biomass mapping from ICESat/GLAS data and MODIS imagery in China. Remote Sens. 7 (5), 5534–5564.

Coops, N.C., 2002. Eucalypt forest structure and synthetic aperture radar backscatter: a theoretical analysis. Trees 16, 28–46. https://doi.org/10.1007/s00468-001-0137-3.

Coops, N.C., Wulder, M.A., Culvenor, D., St-Onge, B., 2004. Comparison of forest attributes extracted from fine spatial resolution multispectral and lidar data. Can. J. Remote. Sens. 30, 855–866.

Cosenza, D.N., Korhonen, L., Maltamo, M., Packalen, P., Strunk, J.L., Næsset, E., Gobakken, T., Soares, P., Tomé, M., 2020. Comparison of linear regression, k-nearest neighbour and random forest methods in airborne laser-scanning-based prediction of growing stock. Forestry. https://doi.org/10.1093/forestry/cpaa034.

Crookston, N.L., Finley, A.O., 2008. yaImpute: an R package for k NN imputation. J. Stat. Softw. 23, 1–16.

Curran, P.J., Atkinson, P.M., 1998. Geostatistics and remote sensing. Prog. Phys. Geogr. 22 (1), 61–78.

De'ath, G., 2002. Multivariate regression trees: a new technique for modelling species–environment relationships. Ecol. 83, 1105–1117.

Degnan, J.J., 2016. Scanning, multibeam, single photon Lidars for rapid, large scale, high resolution, topographic and bathymetric mapping. Remote Sens. 8 (11), 923–958.

Drake, J.B., Dubayah, R.O., Knox, R.G., Clark, D.B., Blair, J.B., 2002. Sensitivity of large-footprint lidar to canopy structure and biomass in a neotropical rainforest. Remote Sens. Environ. 81, 378–392.

Dubayah, R., Blair, J.B., Goetz, S., Fatoyinbo, L., Hansen, M., Healey, S., Hofton, M., Hurtt, G., Kellner, J., Luthcke, S., Armston, J., 2020. The global ecosystem dynamics investigation: high-resolution laser ranging of the Earth's forests and topography. Sci. Remote Sens. 100002.

Duncanson, L., Armston, J., Disney, M., Avitabile, V., Barbier, N., Calders, K., Carter, S., Chave, J., Herold, M., Crowther, T.W., Falkowski, M., Kellner, J.R., Labrière, N., Lucas, R., MacBean, N., McRoberts, R.E., Meyer, V., Næsset, E., Nickeson, J.E., Paul, K.I., Philips, O.L., Réjou-Méchain, M., Román, M., Roxburgh, S., Saatchi, S., Schepaschenko, D., Scipal, K., Siqueira, P.R., Whitehurst, A., Williams, M., 2019. The importance of consistent global forest aboveground biomass product validation. Surv. Geophys. 40 (4), 979–999.

Duncanson, L., Neuenschwander, A., Hancock, S., Thomas, N., Fatoyinbo, T., Simard, M., Silva, C.A., Armston, J., Luthcke, S.B., Hofton, M., Kellner, J., Dubayah, R., 2020. Biomass estimation from simulated GEDI, ICESat-2 and NISAR across environmental gradients in Sonoma County, California. Remote Sens. Environ. 242, 111779.

Eskelson, B.N.I., Temesgen, H., Lemay, V., Barrett, T.M., Crookston, N.L., Hudak, A.T., 2009. The roles of nearest neighbor methods in imputing missing data in forest inventory and monitoring databases. Scand. J. For. Res. 24, 235–246.

Fekety, P.A., Falkowski, M.J., Hudak, A., T., 2015. Temporal transferability of LiDAR-based imputation of forest inventory attributes. Can. J. For. Res. 45 (4), 422–435. https://doi.org/10.1139/cjfr-2014-0405.

Fradette, M.-S., Leboeuf, A., Riopel, M., Bégin, J., 2019. Method to reduce the Bias on digital terrain model and canopy height model from LiDAR data. Remote Sens. 11, 863.

Frazer, G.W., Magnussen, S., Wulder, M.A., Niemann, K., 2011. Simulated impact of sample plot size and co-registration error on the accuracy and uncertainty of LiDAR-derived estimates of forest stand biomass remote Sens. Environ. 115 (2011), 636–649.

Garcia, M., Saatchi, S., Casas, A., Koltunov, A., Ustin, S., Ramirez, C., Garcia-Gutierrez, J., Balzter, H., 2017. Quantifying biomass consumption and carbon release from the California rim fire by integrating airborne LiDAR and Landsat OLI data. J. Geophys. Res. Biogeosci. 122 (2), 340–353.

Goodbody, T.R.H., Coops, N.C., Marshall, P.L., Tompalski, P., Crawford, P., 2017. Unmanned aerial systems for precision forest inventory purposes: a review and case study. For. Chron. 93 (01), 71–81.

Goovaerts, P., 1997. Geostatistics for Natural Resources Evaluation. Oxford University Press on Demand. Oxford University Press, New York, p. 483.

Goward, S.N., Arvidson, T.J., Williams, D.L., Faundeen, J., Irons, J., Franks, S., 2006. Historical record of Landsat global coverage: Mission operations, NSLRSDA, and international cooperator stations. Photogramm. Eng. Remote. Sens. 72, 710–720.

Greene, W.H., 1993. Econometric Analysis, 791. Macmillan Publishing Company, New York.

Hancock, S., Armston, J., Hofton, M., Sun, X., Tang, H., Duncanson, L.I., Kellner, J.R., Dubayah, R., 2019. The GEDI simulator: a large-footprint waveform Lidar simulator for calibration and validation of spaceborne missions. Earth Space Sci. 6 (2), 294–310.

Hartzell, P., Dang, Z., Pan, Z., Glennie, C., 2018. Radiometric evaluation of an airborne single photon LiDAR sensor. IEEE Geosci. Remote Sens. Lett. 15 (9), 1466–1470.

Hawbaker, T.J., Keuler, N.S., Lesak, A.A., Gobakken, T., Contrucci, K., Radeloff, V.C., 2009. Improved estimates of forest vegetation structure and biomass with a LiDAR-optimized sampling design. J. Geophys. Res. Biogeosci. 114, G2.

Hermosilla, T., Wulder, M.A., White, J.C., Coops, N.C., Hobart, G.W., Campbell, L.B., 2016. Mass data processing of time series Landsat imagery: pixels to data products for forest monitoring. Int. J. Digit. Earth. 9, 1035–1054.

Hermosilla, T., Wulder, M.A., White, J.C., Coops, N.C., Hobart, G.W., 2017. Updating Landsat time series of surface-reflectance composites and forest change products with new observations. Int. J. Appl. Earth Obs. Geoinf. 63, 104–111.

Herold, M., Carter, S., Avitabile, Espejo, A. B, Jonckheere, I., Lucas, R., McRoberts, R.E., Næsset, E., Nightingale, J., Petersen, J.R., Romjin, E., Rosenqvist, A., Rozendaal, D. M.A., Seifert, F.M., Sanz, M.J., Sy, V.D., 2019. The role and need for space-based Forest biomass-related measurements in environmental management and policy. Surv. Geophys. 40, 757–778.

Holm, S., Nelson, R., Ståhl, G., 2017. Hybrid three-phase estimators for large-area forest inventory using ground plots, airborne lidar, and space lidar. Remote Sens. Environ. 197, 85–97.

Hudak, A.T., Lefsky, M.A., Cohen, W.B., Berterretche, M., 2002. Integration of lidar and Landsat ETM+ data for estimating and mapping forest canopy height. Remote Sens. Environ. 82 (2), 397–416.

Hudak, A.T., Crookston, M.L., Evans, J.S., Hall, D.E., Falkowski, M.J., 2008. Nearest neighbor imputation of species-level, plot-scale forest structure attributes from LiDAR data. Remote Sens. Environ. 112 (5), 2232–2245.

Hyde, P., Dubayah, R., Walker, W., Blair, J.B., Hofton, M., Hunsaker, C., 2006. Mapping forest structure for wildlife habitat analysis using multi-sensor (LiDAR, SAR/InSAR, ETM+, Quickbird) synergy. Remote Sens. Environ. 102 (1), 63–73.

Kangas, A.S., 1999. Methods for assessing uncertainty of growth and yield predictions. Can. J. For. Res. 29 (9), 1357–1364.

Kellndorfer, J., Walker, W., LaPoint, E., Kirsch, K., Bishop, J., Fiske, G., 2010. Statistical fusion of lidar, InSAR, and optical remote sensing data for forest stand height characterization: a regional-scale method based on LVIS, SRTM, Landsat ETM+, and ancillary data sets. J. Geophys. Res. Biogeosci. 115, G00E08.

Kocev, D., Dzeroski, S., White, M.D., Newell, G.R., Griffioen, P., 2009. Using single-and multi-target regression trees and ensembles to model a compound index of vegetation condition. Ecol. Model. 220 (8), 1159–1168.

Kotivuori, E., Korhonen, L., Packalen, P., 2016. Nationwide airborne laser scanning based models for volume, biomass and dominant height in Finland. Silva Fennica 50 (4), 1–28, 67.

Krige, D.G., 1966. Two-dimensional weighted moving average trend surfaces for ore valuations. Proceedings of symposium on mathematical Statstics and computer applications. Ore Valuation 13–38.

Lefsky, M., 2010. A global forest canopy height map from the moderate resolution imaging Spectroradiometer and the geoscience laser altimeter system. Geophys. Res. Lett. 37 (15).

Lefsky, M.A., Cohen, W.B., Harding, D.J., Parker, G.G., Acker, S.A., 2002. Lidar remote sensing of above-ground biomass in three biomes. Glob. Ecol. Biogeogr. 11, 393–399.

Li, W., Niu, Z., Liang, X., Li, Z., Huang, N., Gao, S., Wang, C., Muhammad, S., 2015. Geostatistical modelling using LiDAR-derived prior knowledge with SPOT-6 data to estimate temperate forest canopy cover and above-ground biomass via stratified random sampling. Int. J. Appl. Earth Obs. Geoinf. 41, 88–98.

Li, W., Li, Z., Niu, Z., Wang, C., Wu, M., Muhammad, S., 2016. Upscaling coniferous forest above-ground biomass based on airborne LiDAR and satellite ALOS PALSAR data. J. Appl. Remote. Sens. 10 (4), 046003.

Lim, K., Treitz, P., Wulder, M.A., St-Onge, B., Flood, M., 2003. LiDAR remote sensing of forest structure. Prog. Phys. Geogr. 27, 88–106.

Luther, J.E., Fournier, R.A., van Lier, O.R., Bujold, M., 2019. Extending ALS-based mapping of forest attributes with medium resolution satellite and environmental data. Remote Sens. 11 (9), 1092.
Magnussen, S., Nord-Larsen, T., Riis-Nielsen, T., 2018. Lidar supported estimators of wood volume and above ground biomass from the Danish national forest inventory (2012–2016). Remote Sens. Environ. 211, 146–153. https://doi.org/10.1016/j.rse.2018.04.015.
Mahoney, C., Hall, R., Hopkinson, C., Filiatrault, M., Beaudoin, A., Chen, Q., 2018. A forest attribute mapping framework: a pilot study in a northern boreal forest, Northwest Territories, Canada. Remote Sens. 10, 1338.
Makela, H., Pekkarinen, A., 2004. Estimation of forest stand volumes by Landsat TM imagery and stand-level field-inventory data. For. Ecol. Manag. 196, 245–255.
Mandlburger, G., Lehner, H., Pfeifer, N., 2019. A comparison of single photon and full waveform lidar. ISPRS Ann. Photogramm. Remote Sens. Spatial Inf. Sci. IV-2/W5, 397–404.
Margolis, H.A., Nelson, R.F., Montesano, P.M., Beaudoin, A., Sun, G., Andersen, H.-E., Wulder, M.A., 2015. Combining satellite lidar, airborne lidar, and ground plots to estimate the amount and distribution of aboveground biomass in the boreal forest of North America. Can. J. For. Res. 45, 838–855.
Markus, T., Neumann, T., Martino, A., Abdalati, W., Brunt, K., Csatho, B., Farrell, S., Fricker, H., Gardner, A., Harding, D., Jasinski, M., Kwok, R., Magruder, D., Lubin, D., Luthcke, S., Morison, J., Nelson, R., Neuenschawander, A., Palm, S., Popescu, S., Shum, C.K., Schutz, B.E., Smith, B., Yang, Y., Jasinski, M., 2017. The ice, cloud, and land elevation Satellite-2 (ICESat-2): science requirements, concept, and implementation. Remote Sens. Environ. 190, 260–273.
Masek, J.G., Vermote, E.F., Saleous, N.E., Wolfe, R., Hall, F.G., Huemmrich, K.F., Gao, F., Kutler, J., Lim, T.K., 2006. A Landsat surface reflectance dataset for North America, 1990-2000. IEEE Geosci. Remote Sens. Lett. 3, 68–72.
Maselli, F., Chiesi, M., Montaghi, A., Pranzini, E., 2011. Use of ETM+ images to extend stem volume estimates obtained from lidar data. ISPRS J. Photogramm. Rem. Sens. 66, 662–671.
Matasci, G., Hermosilla, T., Wulder, M.A., White, J.C., Coops, N.C., Hobart, G.W., Zald, H.S.J., 2018a. Large-area mapping of Canadian boreal forest cover, height, biomass and other structural attributes using Landsat composites and lidar plots. Remote Sens. Environ. 209, 90–106.
Matasci, G., Hermosilla, T., Wulder, M.A., White, J.C., Coops, N.C., Hobart, G.W., Bolton, D.K., Tompalski, P., Bater, C.W., 2018b. Three decades of forest structural dynamics over Canada's forested ecosystems using Landsat time-series and lidar plots. Remote Sens. Environ. 216, 697–714.
McInerney, D.O., Suarez-Minguez, J., Valbuena, R., 2010. Nieuwenhuis, M. Forest canopy height retrieval using LiDAR data, medium-resolution satellite imagery and kNN estimation in Aberfoyle. Scotland. Forestry. 83, 195–206.
McRoberts, R.E., Næsset, E., Gobakken, T., Chirici, G., Condés, S., Hou, Z., Saarela, S., Qi, C., Ståhl, S., Walters, B.F., 2018. Assessing components of model-based mean square error estimator for remote sensing assisted forest applications. Can. J. For. Res. 48, 642–649.
Melo, L., Schneider, R., Fortin, M., 2018. Estimating model-and sampling-related uncertainty in large-area growth predictions. Ecol. Model. 390, 62–69.
Miller, J.R., Turner, M.G., Smithwick, E.A.H., Dent, C.L., Stanley, E.H., 2004. Spatial extrapolation: the science of predicting ecological patterns and processes. Biosci. 54 (4), 310–320.
Montesano, P.M., Cook, B.D., Sun, G., Simard, M., Nelson, R.F., Ranson, K.J., Zhang, Z., Luthcke, S., 2013. Achieving accuracy requirements for forest biomass mapping: a spaceborne data fusion method for estimating forest biomass and LiDAR sampling error. Remote Sens. Environ. 130, 153–170.
Næsset, E., 2002. Predicting forest stand characteristics with airborne scanning laser using a practical two-stage procedure and field data. Remote Sens. Environ. 80, 88–99.
Næsset, E., 2014. Area-based inventory in Norway – from innovation to an operational reality. In: Maltamo, M., Næsset, E., Vauhkonen, J. (Eds.), For Appl Airborne Laser Scanning Concepts Case Stud. Springer Netherlands, Dordrecht, pp. 215–240.
Næsset, E., Bollandsas, O.M., Gobakken, T., Gregoire, T.G., Stahl, G., 2013. Model-assisted estimation of change in forest biomass over an 11 year period in a sample survey supported by airborne LiDAR: a case study with post-stratification to provide "activity data". Remote Sens. Environ. 128, 299–314.
Neigh, C.S., Nelson, R.F., Ranson, K.J., Margolis, H.A., Montesano, P.M., Sun, G., Kharuk, V., Næsset, E., Wulder, M.A., Andersen, H.-E., 2013. Taking stock of circumboreal forest carbon with ground measurements, airborne and spaceborne lidar. Remote Sens. Environ. 137, 274–287.
Nelson, R., 2013. How did we get here? An early history of forestry lidar. Can. J. Remote. Sens. 39 (sup1), S6–S17.
Nelson, R., Boudreau, J., Gregoire, T.G., Margolis, H.A., Næsset, E., Gobakken, T., Ståhl, G., 2009. Estimating Quebec provincial forest resources using ICESat/GLAS. Can. J. For. Res. 39, 862–881.
Neuenschwander, A., Magruder, L., 2019. Canopy and terrain height retrievals with ICESat-2: a first look. Remote Sens. 2019 (11), 1721.
Neuenschwander, A., Pitts, K., 2019. The ATL08 land and vegetation product for the ICESat-2 mission. Remote Sens. Environ. 221, 247–259.
Neuenschwander, A.L., Pitts, K.L., Jelley, B.P., Robbins, J., Klotz, B., Popescu, S.C., Nelson, R.F., Harding, D., Pederson, D., Sheridan, R., 2020. ATLAS/ICESat-2 L3A Land and Vegetation Height, Version 3. Boulder, Colorado USA. NASA National Snow and Ice Data Center Distributed Active Archive Center. https://doi.org/10.5067/ATLAS/ATL08.003 [Data accessed April 2020].
Neumann, T.A., Martino, A.J., Markus, T., Bae, S., Bock, M.R., Brenner, A.C., Brunt, K.M., Cavanaugh, J., Fernandes, S.T., Hancock, D.W., Harbeck, K., Lee, J., Kurtz, N.T., Luers, P.J., Luthcke, S.B., Magruder, L., Pennington, T.A., Ramos-Izquierdo, L., Rebold, T., Skoog, J., Thomas, T.C., 2019. The ice, cloud, and land elevation satellite–2 mission: a global geolocated photon product derived from the advanced topographic laser altimeter system. Remote Sens. Environ. 233, 111325.
Packalén, P., Temesgen, H., Maltamo, M., 2012. Variable selection strategies for nearest neighbor imputation methods used in remote sensing based forest inventory. Can. J. Remote. Sens. 38 (05), 557–569.
Pascual, C., García-Abril, A., Cohen, W.B., Martín-Fernández, S., 2010. Relationship between LiDAR-derived forest canopy height and Landsat images. Int. J. Remote Sens. 31 (5), 1261–1280.
Patterson, P., Healey, S., Stahl, G., Saarela, S., Holm, S., Andersen, H.-E., Dubahay, D.O., Duncanson, L., Hancock, S., Armston, J., Kellner, J.R., Cohen, W.B., Yang, Z., 2019. Statistical properties of hybrid estimators proposed for GEDI-NASA's global ecosystem dynamics investigation. Environ. Res. Lett. 14 (6).
Penner, M., Pitt, D.G., Woods, M.E., 2013. Parametric vs. nonparametric LiDAR models for operational forest inventory in boreal Ontario. Can. J. Remote. Sens. 39, 426–443.
Pflugmacher, D., Cohen, W.B., Kennedy, R., 2012. Using Landsat-derived disturbance history (1972–2010) to predict current forest structure. Remote Sens. Environ. 122, 146–165.
Phillips, D.L., Brown, S.L., Schroeder, P.E., Birdsey, R., 2000. Toward error analysis of large scale forest carbon budgets. Glob. Ecol. Biogeogr. 9, 305–313.
Pitkänen, T.P., Käyhkö, N., 2017. Reducing classification error of grassland overgrowth by combing low-density lidar acquisitions and optical remote sensing data. ISPRS J. Photogram. Rem. Sens. 130, 150–161.
Puliti, S., Saarela, S., Gobakken, T., Ståhl, G., Næsset, E., 2018. Combining UAV and Sentinel-2 auxiliary data for forest growing stock volume estimation through hierarchical model-based inference. Remote Sens. Environ. 204, 485–497.
Queinnec, M., Tompalski, P., Bolton, D.K., Coops, N.C., 2020. FOSTER—an R package for forest structure extrapolation. PLoS One 16 (1), e0244846.
Réjou-Méchain, M., Barbier, N., Couteron, P., Ploton, P., Vincent, G., Herold, M., Mermoz, S., Saatchi, S., Chave, J., de Boissieu, F., Féret, J.-B., Momo Takoudjou, S., Pélissier, R., 2019. Upscaling forest biomass from field to satellite measurements: sources of errors and ways to reduce them. Surv. Geophys. 1–31.
Saarela, S., Holm, S., Grafström, A., Schnell, S., Næsset, E., Gregoire, T.G., Nelson, R.F., Ståhl, G., 2016. Hierarchical model-based inference for forest inventory utilizing three sources of information. Ann. For. Sci. 73, 895–910.
Saarela, S., Holm, S., Healey, S., Andersen, H.-E., Petersson, H., Prentius, W., Patterson, P., Næsset, E., Gregoire, T., Ståhl, G., 2018. Generalized hierarchical model-based estimation for AbovegroundBiomass assessment using GEDI and Landsat data. Remote Sens. 10, 1832.
Saarela, S., Holm, S., Yang, Z., 2020a. HMB: Hierarchical Model-Based Estimation Approach. R Package Version 1.1. https://CRAN.R-project.org/package=HMB.
Saarela, S., Wästlund, A., Holmström, E., Appiah Mensah, A., Holm, S., Nilsson, M., Fridman, J., Ståhl, G., 2020b. Mapping aboveground biomass and its prediction uncertainty using LiDAR and field data, accounting for tree-level allometric and LiDAR model errors. For. Ecosystems. 7, 43.
Simard, M., Pinto, N., Fisher, J.B., Baccini, A., 2011. Mapping forest canopy height globally with spaceborne lidar. J. Geophys. Res. 116 (G4).
Ståhl, G., Saarela, S., Schnell, S., Holm, S., Breidenbach, J., Healey, S.P., Patterson, P.L., Magnussen, S., Naesset, E., McRoberts, R.E., Gregoire, T.G., 2016. Use of models in large-area forest surveys: comparing model-assisted, model-based and hybrid estimation. For Ecosystems. 3 (1), 5.
Stojanova, D., Panov, P., Gjorgjioski, V., Kobler, A., Džeroski, S., 2010. Estimating vegetation height and canopy cover from remotely sensed data with machine learning. Ecol. Info. 5 (4), 256–266.
Strunk, J.L., Temesgen, H., Andersen, H., Packalen, P., 2014. Prediction of Forest attributes with field plots, Landsat, and a sample of Lidar strips: a case study on the Kenai peninsula, Alaska. Photogramm. Eng. Remote. Sens. 143–150.
Sun, G., Ranson, K.J., Guo, Z., Zhang, Z., Montesano, P., Kimes, D., 2011. Forest biomass mapping from lidar and radar synergies. Remote Sens. Environ. 115 (11), 2906–2916.
Swatantran, A., Tang, H., Barrett, T., Decola, P., Dubayah, R., 2016. Rapid, high-resolution forest structure and terrain mapping over large areas using single photon lidar. Sci. Rep. 6, 28277.
Tompalski, P., Rakofsky, J., Coops, N.C., White, J.C., Graham, A.N., Rosychuk, R., 2019. Challenges of multi-temporal and multi-sensor forest growth analyses in a highly disturbed boreal mixedwood forests. Remote Sens. 11 (18), 2102.
Tomppo, E., Olsson, H., Ståhl, G., Nilsson, M., Hagner, O., Katila, M., 2008. Combining national forest inventory field plots and remote sensing data for forest databases. Remote Sens. Environ. 112, 1982–1999.
Tsui, O.W., Coops, N.C., Wulder, M.A., Marshall, P.L., 2013. Integrating airborne LiDAR and space-borne radar via multivariate kriging to estimate above-ground biomass rem. Sens. Environ. 139, 340–352.
Urbazaev, M., Thiel, C., Cremer, F., Dubayah, R., Migliavacca, M., Reichstein, M., Schmullius, C., 2018. Estimation of forest aboveground biomass and uncertainties by integration of field measurements, airborne LiDAR, and SAR and optical satellite data in Mexico. Carbon Bal. Manag. 13.
Wang, Y., Lehtomäki, M., Liang, X., Pyörälä, J., Kukko, A., Jaakkola, A., Hyyppä, J., 2019. Is field-measured tree height as reliable as believed – a comparison study of tree height estimates from field measurement, airborne laser scanning and terrestrial laser scanning in a boreal forest. ISPRS J. Photogramm. Remote Sens. https://doi.org/10.1016/j.isprsjprs.2018.11.008.
Wästlund, A., Holmgren, J., Lindberg, E., Olsson, H., 2018. Forest variable estimation using a high altitude single photon Lidar system. Remote Sens. 10, 1422.
Webster, R., 1985. Quantitative spatial analysis of soil in the field. Springer-Verlag. 3, 1–70.

White, J.C., Wulder, M.A., Varhola, A., Vastaranta, M., Coops, N.C., Cook, B.D., Pitt, D., Woods, M., 2013. A best practices guide for generating forest inventory attributes from airborne laser scanning data using an area-based approach. For. Chron. 89, 722–723.

White, J.C., Wulder, M.A., Hobart, G.W., Luther, J.E., Hermosilla, T., Griffiths, P., Coops, N.C., Hall, R.J., Hostert, P., Dyk, A., Guindon, L., 2014. Pixel-based image compositing for large-area dense time series applications and science. Can. J. Remote. Sens. 40, 192–212.

White, J.C., Coops, N.C., Wulder, M.A., Vastaranta, M., Hilker, T., Tompalski, P., 2016. Remote sensing Technologies for Enhancing Forest Inventories: a review. Can. J. Remote. Sens. 42, 619–641.

White, J.C., Tompalski, P., Vastaranta, M., Wulder, M.A., Saarinen, S., Stepper, C., Coops, N.C., 2017. A model development and application guide for generating an enhanced forest inventory using airborne laser scanning data and an area-based approach. In: CWFC Information Report FI-X-018, Canadian Forest Service. Pacific Forestry Centre, Victoria, BC, Canada, p. 38.

Wulder, M.A., Coops, N.C., 2014. Satellites: make earth observations open access. Nature. 513, 30–32.

Wulder, M.A., White, J.C., Goward, S.N., Masek, J.G., Irons, J.R., Herold, M., Cohen, W. B., Loveland, T.R., Woodcock, C.E., 2008. Landsat continuity: issues and opportunities for land cover monitoring. Remote Sens. Environ. 112, 955–969.

Wulder, M.A., White, J.C., Nelson, R.F., Næsset, E., Ørka, H.O., Coops, N.C., Hilker, T., Bater, C.W., Gobakken, T., 2012a. Lidar sampling for large-area forest characterization: a review. Remote Sens. Environ. 121, 196–209.

Wulder, M.A., White, J.C., Bater, C.W., Coops, N.C., Hopkinson, C., Chen, G., 2012b. Lidar plots - a new large-area data collection option: context, concepts, and case study. Can. J. Remote. Sens. 38, 600–618.

Wulder, M.A., Masek, J., Cohen, W., Loveland, T., Woodcock, C., 2012c. Opening the archive: how free data has enabled the science and monitoring promise of Landsat. Remote Sens. Environ. 122, 2–10.

Wulder, M.A., Coops, N.C., Hudak, A.T., Morsdorf, F., Nelson, R., Newnham, G., Vastaranta, M., 2013. Status and prospects for LiDAR remote sensing of forested ecosystems. Can. J. Remote. Sens. 39, S1–S5.

Wulder, M.A., Hermosilla, T., White, J.C., Coops, N.C., 2020. Biomass status and dynamics over Canada's forests: disentangling disturbed area from associated aboveground biomass consequences. Environ. Res. Lett. 15, 094093.

Zald, H.S.J., Wulder, M.A., White, J.C., Hilker, T., Hermosilla, T., Hobart, G.W., Coops, N.C., 2016. Integrating Landsat pixel composites and change metrics with lidar plots to predictively map forest structure and aboveground biomass in Saskatchewan, Canada. Remote Sens. Environ. 176, 188–201.

Zhu, Z., Woodcock, C.E., 2014. Automated cloud, cloud shadow, and snow detection in multitemporal Landsat data: an algorithm designed specifically for monitoring land cover change. Remote Sens. Environ. 152, 217–234.